

Experimental Investigation of Savonius Wind Rotors in Open and Bounded Flows

By

Goh Jin Ming

Dissertation submitted in partial fulfilment of
the requirements for the
Bachelor of Engineering (Hons)
(Mechanical Engineering)

MAY 2011

Universiti Teknologi Petronas
Bandar Seri Iskandar
31750 Tronoh
Perak Darul Ridzuan

CERTIFICATION OF APPROVAL

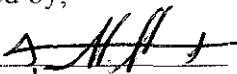
Experimental Investigation of Savonius Wind Rotors in Open and Bounded Flows

By

Goh Jin Ming

A project dissertation submitted to the
Mechanical Engineering Programme
Universiti Teknologi PETRONAS
in partial fulfilment of the requirement for the
BACHELOR OF ENGINEERING (Hons)
(MECHANICAL ENGINEERING)

Approved by,



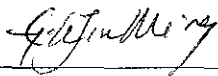
(Name of Main Supervisor)

UNIVERSITI TEKNOLOGI PETRONAS
TRONOH, PERAK

January 2006

CERTIFICATION OF ORIGINALITY

This is to certify that I am responsible for the work submitted in this project, that the original work is my own except as specified in the references and acknowledgements, and that the original work contained herein have not been undertaken or done by unspecified sources or persons.



GOH JIN MING

ABSTRACT

The common practice of operating a Savonius rotor is in an open environment; however there are times when the rotor is fixed in a bounded environment and there might be changes in the performance of the rotor. The project aims to investigate the possible changes in the performance of the rotor. Three different rotors models are design in this project. The project is conducted experimentally to compare the performance of the Rotors in bounded environment against open environment. The different environments that are tested namely partially bounded environment, fully bounded environment and open environment. Rotors are found to have better starting capabilities when operated in bounded environment, Rotor 1 starts at 1.7m/s and 2m/s in partially bounded environment and fully bounded environment as compared to 2.7m/s in open environment. Rotor 2 starts at approximately 3.4 m/s for both partially and fully bounded environment as compared to open environment. Rotor 3 starts at 2m/s and 1.8m/s for partially bounded and fully bounded environment as compared to 3m/s for open environment. Apart from that, all rotors manage to achieve higher power coefficient at a higher TSR as compare to open environment and better torque coefficient as well in bounded environment as compare to open environment.

TABLE OF CONTENT

	Page
ABSTRACT	i
CHAPTER 1:INTRODUCTION	1
1.1 Background	1
1.2 Problem Statement	3
1.3 Objectives	3
1.4 Scope of Work	3
CHAPTER 2: LITERATURE REVIEW	4
CHAPTER 3: METHODOLOGY	12
3.1 Analysis Technique	12
3.2 Tools/Equipment Required	12
3.3Software Required	12
3.4 Design and Fabricate Models	13
3.4.1 Design Constraints	13
3.4.2 Design Criteria	14
3.4.3 Material Selection	15
3.4.4 Dimensional Analysis	16
3.4.5 Prototype Design	19
3.4.6 Fabrication of Rotor	19
3.5 Design and Fabricate Experimental Test Rig	20
3.5.1 Test Rig Design	20
3.5.2 Material Selection	22
3.5.3 Fabrication of Test Rig	22
3.6 Experimental Procedure	24
3.7 Flow Chart	26
3.8 Gantt Chart	27

CHAPTER 4:	RESULT AND DISCUSSION	29
4.1	Data Gathering and Analysis	29
4.2	Results and Discussion	36
4.2.1	Comparison between Rotors	36
4.2.2	Comparison between Operating Environments Rotor1	37
4.2.3	Comparison between Operating Environments Rotor2	39
4.2.4	Comparison between Operating Environments Rotor3	40
CHAPTER 5:	CONCLUSION & RECOMMENDATION	40
5.1	Conclusion	42
5.2	Recommendation	43
REFERENCES		45
APPENDICES		47

LIST OF FIGURES

PAGE

Figure 1.1: Off Shore Wind Farm in the North Sea of Belgium	1
Figure 1.2: Schematic Drawing of a Conventional Savonius Turbine	2
Figure 1. 3: Operation of a Savonius Wind Turbine	2
Figure 2.1: Description, parameters characterizing two blades S-Rotor	4
Figure 2.2: Description of the geometry and free optimization parameters	5
Figure 2.3: Basic modified Savonius rotor without shaft	7
Figure 2.4: Curtain arrangement placed in front of the Savonius wind rotor	8
Figure 2.5: Schematic diagram of experimental set up	8
Figure 2.6: Schematic view of experimental apparatus with Guide Box Tunnel	9
Figure 2.7: Optimum configuration, through optimization procedures	9
Figure 2.8: Flow pattern across the twisted blade	10
Figure 2.9: Influence of Reynolds number on the aerodynamic coefficient	11
Figure 3.1: Schematic Dimension of Two Bladed Rotors	14
Figure 3.2: Dimensional Analysis of Blade Design 2	17
Figure 3.3: Top View of Design 3	18
Figure 3.4: Side View of Design 3	19
Figure 3.5: From Left to Right Prototype Rotor 1, 2 and 3	20
Figure 3.6: Attachment of Low Friction Bearing to Rotor Shaft	20
Figure 3.7: Partially Bounded Casing	21
Figure 3.8: Partially Bounded Casing	21
Figure 3.9: Fabricated Partially Bounded Casing	23
Figure 3.10: Front View of Fabricated Partially Bounded Casing	23
Figure 3.11: Fabricated Fully Bounded Casing	23
Figure 3.12: Experiment Set Up	23
Figure 3.13: Flow Chart for Final Year Project	26
Figure 3.14: Gantt chart for Final Year Project 1	27
Figure 3.15: Gantt chart for Final Year Project 2	28
Figure 4.1: The Power Coefficient versus TSR for Rotors	36

Figure 4.2: The Torque Coefficient versus TSR of Rotors	36
Figure 4.3: C_p Comparison between Operating Environments of Rotor 1	37
Figure 4.4: C_T Comparison between Operating Environments of Rotor 1	38
Figure 4.5: C_p Comparison between Operating Environments of Rotor 2	39
Figure 4.6: C_T Comparison between Operating Environments of Rotor 2.	39
Figure 4.7: C_p Comparison between Operating Environments for Rotor 3	40
Figure 4.8: C_T Comparison between Operating Environment for Rotor 3	41

LIST OF TABLES	PAGE
Table 2.1: Performance of Savonius Rotor System	6
Table 2.2: Optimal values for main geometrical parameters	11
Table 3.1: Pugh Selection Matrix for End Plate's Material	15
Table 3.2: Pugh Selection Matrix for Rotor Blade's Material	15
Table 3.3: Pugh Selection Matrix for Test Rig's Material	22
Table 4.1: Data for Wind Speed, Rotor Rotational Speed and Torque in Open Environment	30
Table 4.2: Data for Wind Speed, Rotor Rotational Speed, Torque in Partially Bounded Environment	31
Table 4.3: Data for Wind Speed, Rotor Rotational Speed, Torque in Fully Bounded Environment	32
Table 4.4: Results for Rotor 1, 2 and 3 in Open Environment	33
Table 4.5: Results for Rotor 1, 2 and 3 in Partially Bounded Environment	34
Table 4.6: Results for Rotor 1, 2 and 3 in Fully Bounded Environment	35

CHAPTER 1

INTRODUCTION

1.1 Background

Ever since the worldwide energy crisis strikes, people around the world has move out to search for alternative and renewable energy sources. Wind energy has become a particularly interesting field for scientist and engineers to work in. As of today, we have wind turbines placed around the globe to harvest wind energy and most of the time what we get to see are horizontal axis wind turbines utilizes in most of the wind farm around the globe. Despite, the fact that horizontal wind turbines are good alternatives for harvesting renewable energy source, they are still relatively expensive and difficulties in installation and transportation as well as subjected to places with strong wind forces.

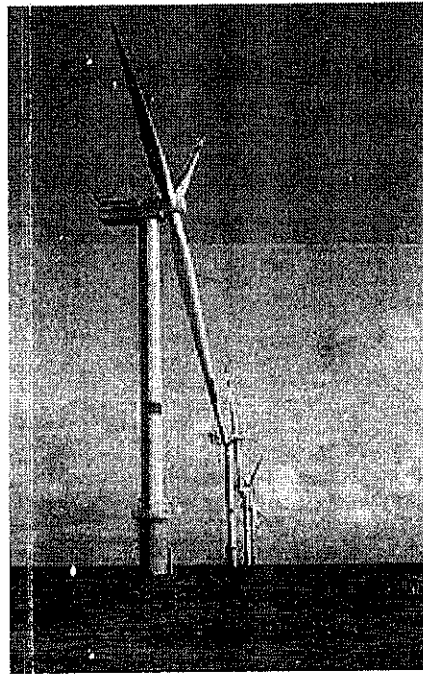


Figure 1.1: Off Shore Wind Farm in the North Sea of Belgium ^{Ref[1]}

In 1922, a French engineer name S.J Savonius developed a vertical axis Savonius rotor. The concept of the conventional Savonius rotor is based on cutting a cylinder into two halves along the cutting plane, so that the cross-section resembles the letter S. The Savonius turbine is simpler than the conventional horizontal axis wind turbine. In the sense of aerodynamically, the two curvatures of the halves is then place in such a way that, it forms an S curvature and utilizes the drag force of the wind which

is why the rotor experiences less drag when moving against the wind than with the wind, hence leads to the spin of the rotor.

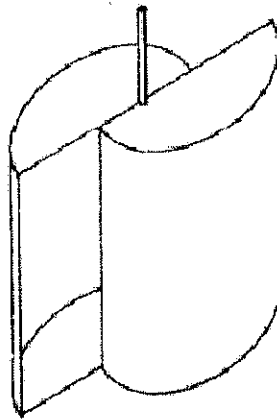


Figure 1.2: Schematic Drawing of a Conventional Savonius Turbine^{Ref [2]}

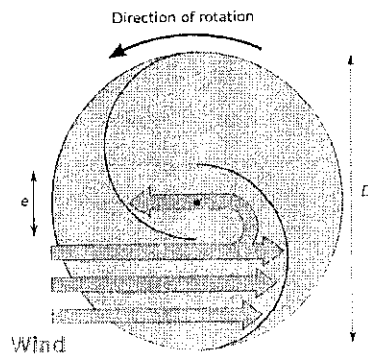


Figure 1.3: Operation of a Savonius Wind Turbine^{Ref [2]}

However, both the horizontal and vertical axis wind turbines have a flaw when operates in open flows. When flow of wind approaches a wind rotor, most of the flow rate is deviated to the sides of the rotor. Hence, it has come to attention that if the rotors are installed in a bounded configuration, the side escape of the flow reduces considerably and so increases the power coefficient as well.

1.2 Problem Statement

The performance of the wind rotors are usually examined in open atmosphere. For some applications, the rotor is installed inside bounded boundaries. The power coefficient will differ and needs to be evaluated experimentally.

1.3 Objectives

The objectives of the project are:

- a. To determine different types of S-Rotors in unbounded operation.
- b. To determine the performance of the selected rotors in (a) and also in bounded operation.

1.4 Scope of Work

In this project, the aim is to investigate the possible enhancement of power coefficient of three different Savonius rotor designs in partially bounded flow and fully bounded flow against open environment. The scopes of work included in this project are:

- a. To design prototype that are able to test the Savonius rotor in three different design and configuration of open environment, partially bounded flow and fully bounded flow.
- b. To find ways to fabricate the approve designs.
- c. To perform experimental analysis on the fabricated prototype by comparing the enhancement of power coefficient when running in partially bounded surface and fully bounded surface against open environment.

CHAPTER 2

LITERATURE REVIEW

In Ref [3], the research is a numerical study on optimization of Savonius turbines using an obstacle shielding the returning blade. The research is done based on the understanding that by adding a shielding plate at the front of the returning plate, the reverse moment created by the returning plate will be reduced and hence the total moment of the turbine will increase comparing the Savonius turbines with no shielding effect as the total moment would be the subtraction between the advancing moment against the returning moment. The work is to look into details the optimization of angles and position of the shielding plate. What is relevant from the research done, is that the design configuration of the blades that are utilized in the research work can be implemented in current project work, which in this case conventional Savonius geometry, meaning that the geometrical parameters of 'a' and 'e' are always fixed and respectively equal to 0 and $R/3$.

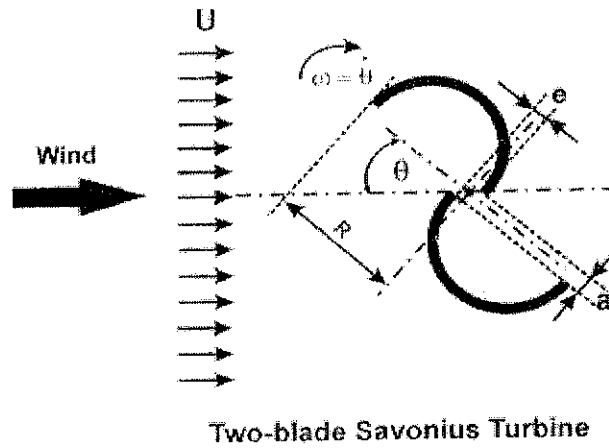


Figure 2.1: Description, parameters characterizing a two blade S- Rotor. ^{Ref[3]}

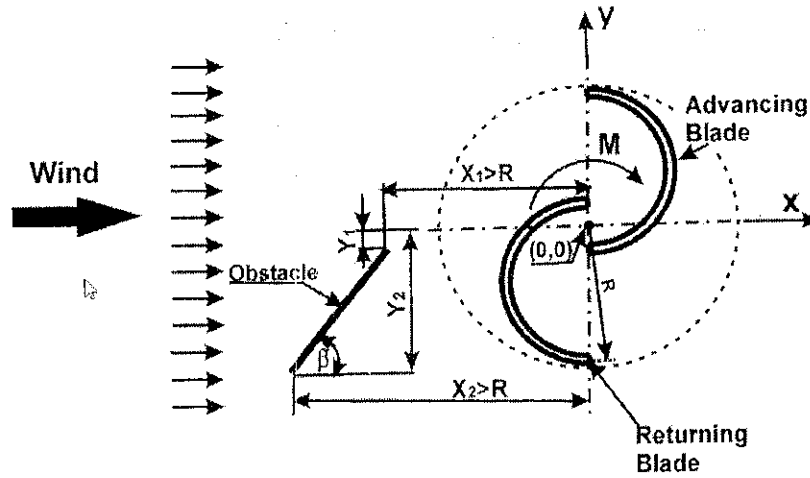


Figure 2.2: Description of the geometry and free optimization parameters. ^{Ref[3]}

The important things to note about the research work is of course the increase self starting capability of the Savonius rotor. The negative torque region has been completely eliminated with the introduction of obstacle shielding plate and the ideal position of the shielding plate is listed in the paper and β is found to be ideal at 100.8° and the reason is partially shown in the paper and can be understand well after careful analyzing. The research had found a considerable increase of power output coefficient of about 27.3% for the two blades Savonius rotor comparing to conventional Savonius rotor without obstacle shielding.

In the research work done on Ref [4], optimization work is carried out on the design configuration of Savonius rotor through wind tunnel experiments. Experiment works are carried out on Savonius rotor in order to optimize the different parameters like number of stages, number of blades and the geometry of the blade, whether or not it is in semicircular shape or twisted. Apart from that, the articles also discussed about the optimum design of blades and end plates which can be useful towards building my prototype later on. The research work found out that, the optimum number of blades for a Savonius Turbine is two whether or not it is in single, two or three stage system. Comparing to a semicircular geometry blade, the twisted geometry has a better performance. Apart from that two is the optimum number of stages for a Savonius rotor system. However, when there is a valve design on the blades, the power coefficient increases on three blade rotors comparing to the conventional three blade design. The reason two stages is better than three is because of the

increase of inertia on the rotor. For the reason two blades are better than three blades is because when the air strikes on one blade get reflected, it hits on the other blades and you have a negative moment.

Table 2.1: Performance of Savonius Rotor System ^{Ref [4]}

Rotor system	No. of blades	Blade shape	Blade height (m)	Blade chord (m)	Aspect ratio	Projected area (m ²)	Free stream velocity (m/s)	Max. power coefficient (C _p)
Single-stage	2	Semicircular	0.173	0.109	1.58	0.0377	8.23	0.18
		Twisted						0.19
	3	Semicircular						0.15
		Twisted						0.16
Two-stage	2	Semicircular	0.122	0.077	1.58	0.0377	7.30	0.29
		Twisted						0.31
	3	Semicircular						0.26
		Twisted						0.28
Three-stage	2	Semicircular	0.100	0.063	1.58	0.0377	8.23	0.23
		Twisted						0.24
	3	Semicircular						0.20
		Twisted						0.21

The study has been extremely helpful to my future work especially on my prototype design. Even thou my main objectives are to compare to power coefficient on the Savonius rotor on bounded and unbounded operation, the details given in the design of the research can serve as a basis for my design of prototype.

In the research article of M.A.Kamoji [5] and partners, they are trying to investigate the improvement in coefficient of power and to obtain the coefficient of static torque by studying and performing experiment on the conventional and modified Savonius rotor with shaft and without shaft in an open jet wind tunnel. The parameters that of concern are overlap ratio, blade arc angle, aspect ratio and Reynolds number. The studied of modified Savonius rotor with shaft is based on the optimum geometry reported by previous researcher, Modi and Fernando [6]. The research found that, the power coefficient is best for modified Savonius Rotor without shaft.

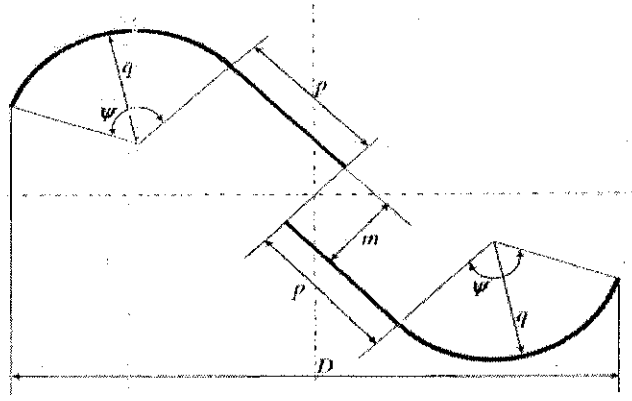


Figure 2.3: Basic modified Savonius rotor without shaft. ^{Ref [5]}

The optimum configuration of modified blade geometry was, overlap ratio equals to zero, aspect ratio of 0.7, blade arc angle of 124° and end plate parameters of 1.1 produce highest coefficient of power. The propose geometry will serve as a reference for current project rotor design.

Apart from that the research work had given a lot of good inputs on blades, end plate materials and also the setting up of housing for the experiment. The results of the research work will also be served as a comparison with project results.

Burçin Deda Altan and Mehmet Atılğan [7] conducted a study on the use of curtaining to increase the performance level of Savonius rotor. The reason being that, the curtain helps to direct the flow of wind into the concave blade and also to prevent a negative torque created as the wind hit the convex blade. Apart from that, the curtaining also helps to increase the velocity of air that hits the concave surface of the Savonius rotor. They tested out the curtaining in three different dimensions and the best curtain angles are found through numerical analysis and experimental analysis. The metal sheet is made from flat metal sheets and so do the end plates and the rotor blades. The design of the curtain arrangement and the schematic arrangement of the experiment are as below.

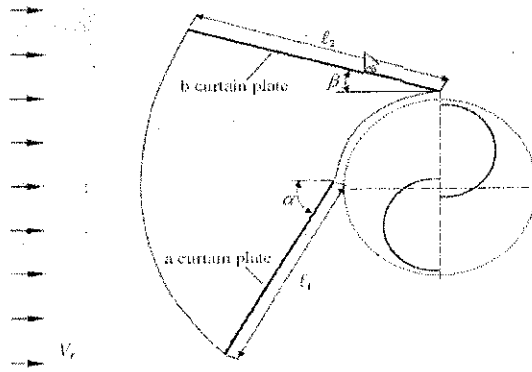


Figure 2.4: Curtain arrangement placed in front of the Savonius wind rotor. Ref [7]

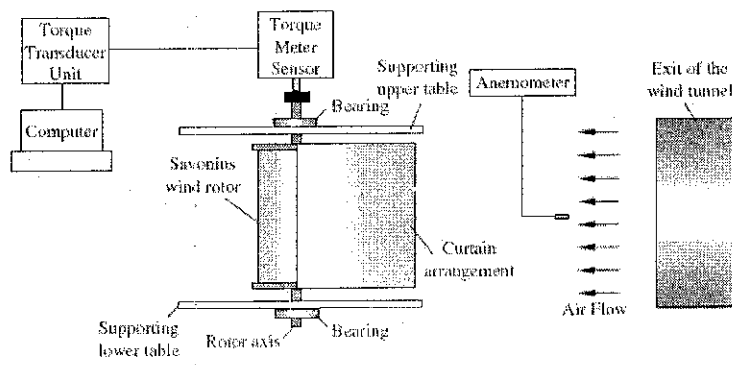


Figure 2.5: Schematic diagram of experimental set up. Ref [7]

In this arrangement α and β represents the angle for the curtain plates while l_1 and l_2 represents the length of the curtain plates. The research work found that the best torque values have been obtained from curtain 1, which have the longest plate for both and it has been indicated through experiments and numerical analysis that for α at 45° and β at 15° the best performance was achieved when rotor blade. The design of the curtain arrangement could be useful for my design of bounded flow operation; the front guiding plates can utilize the angle of degree for both α and β .

Kunio Irabu and Jitendro Nath Roy [8] conducted a study on characteristics of wind power on Savonius rotor using a guide box tunnel. The initial idea of the study was to investigate ways to improve and adjust the output power of Savonius rotor under various wind power and to prevent rotor from strong wind disaster. However, at the end of the study, they found out that the guide box tunnel is capable of increasing the rotor rotational speed and hence the value of output efficiency is higher compare to Savonius rotor without guide box tunnel. The performance of the Savonius rotor with guide box tunnel is comparable enough with other methods and augmentation and

control of the output. The research discuss about the suitable dimensions of constructing a guide box tunnel which can be useful for references when designing a bounded area for the test rig of Savonius rotor. However, there has a slight problem with the design as in certain angle of the rotor; there might be negative starting capability. And apart from that winds are allow escaping from the side of the wall. It was found that the optimum value of spacing ratio between the rotor tip and the side walls are 1.4, with the presence of guide box tunnel the two blades provides larger output power coefficient as compare to the three blades, however both design with guide box tunnel has better coefficient of power as compare to non guide box tunnel design.

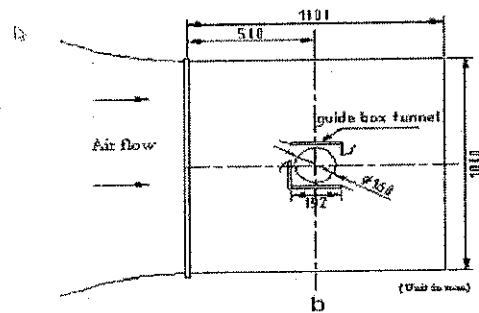


Figure 2.6: Schematic view of experimental apparatus with Guide Box Tunnel. ^{Ref [8]}

In Ref [9], the research work is an advance from the previous work of obstacle shielding but with improves blade shape. The work is main numerical optimization work and non experimental work was carried out. The study aims to improve the output power of Savonius rotor as well as the static torque, which measures the self starting capability of the rotor. With the improve designs of blade shape, the performance exceeds 30% throughout the useful operating range, and the static torque is found to be positive at any angle and is capable of self starting.

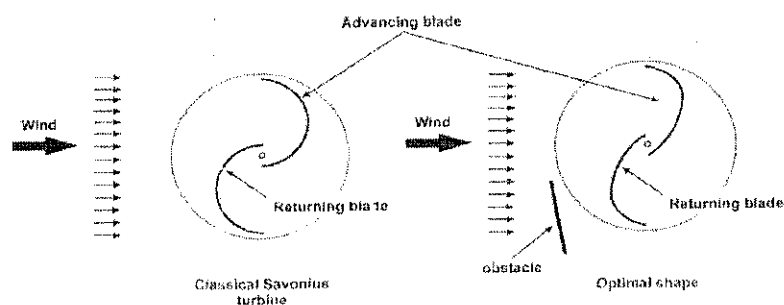


Figure 2.7: Optimum configuration, through optimization procedures. ^{Ref [9]}

Of course there isn't much relevancy to the project as the objectives is just to compare the power coefficient in bounded flows operation and unbounded flows operation, but is good to know that with such improves design, the starting capabilities of the rotor can be improve. However, the cost of manufacturing the blades would be higher but the result will outweigh the cost of the manufacturing.

In the research work conducted by A.S Grinspan and colleagues, Ref [10], they try to investigate performance characteristics of different types of lade shapes which are curved, straight, aerofoil and twisted. Is found that the twisted blade shape has the best performance coefficient compare to the other blade types, however the cost effectiveness has to be studied by actual field test. The reason why twisted blades are better are because it decreases negative wetted area, reduce negative torque by the twist of blade, and it has good self starting capabilities.

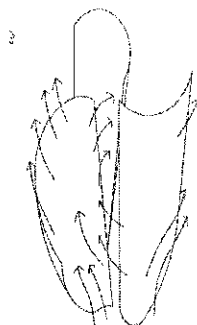


Figure 2.8: Flow pattern across the twisted blade.^{Ref[10]}

It is good to take note about the advantages of twisted blades as it could be use for further studies in bounded flow operations and there might be higher possibilities in increasing the efficiency if my work is found to be successful. Apart from that, the designs or setting up of the housing can also be use in my design considerations.

In the work done by Jean-Luc Menet and colleague Ref [11], the optimal geometrical parameters of the rotor, the influence of a central shaft, the presence and geometry of external chassis and the influence of Reynolds's number are investigated. The results of optimum geometrical parameters are shown in table below.

Table 2.2: Optimal values for main geometrical parameters.^{Ref[11]}

Number of steps	Number of paddles	End-plates radius R_f	Height of the rotor H	Primary overlap e	Secondary overlap a
$2 \rightarrow \infty$	≥ 2	$1.1 R$	$4 R$	$0.15 d \rightarrow 0.3 d$	0

The numerical studies also confirm that the conventional value for the overlap ratio 0.242 is an optimal value. The presence of shafts and external chassis does not influence much on the output power coefficient of the rotor. Reynolds's numbers results are compiled in figure below.

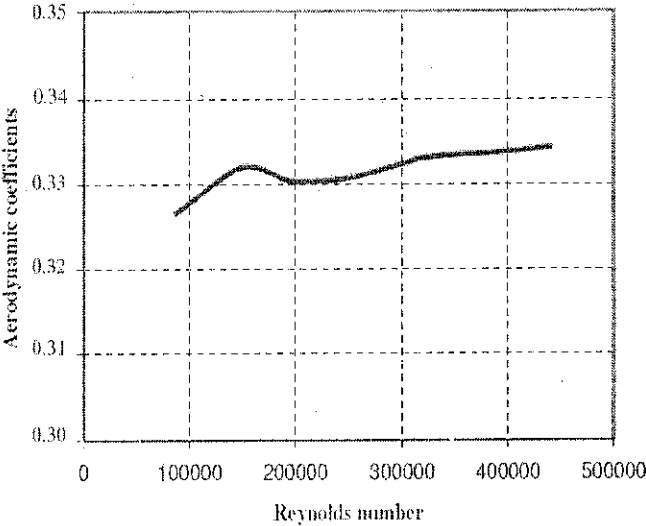


Figure 2.9: Influence of Reynolds number on the aerodynamic coefficient. ^{Ref [11]}

CHAPTER 3

METHODOLOGY

3.1 Analysis Technique

The analysis techniques that are required in the project of experimental investigation of wind rotors in open, partially bounded and fully bounded flows is:

1. Experimental

3.2 Tools/Equipment Require

1. Torque Meter
2. Tachometer
3. Vane Anemometer
4. Portable Industrial Fan

3.3 Software Require

1. AutoCAD
2. Microsoft Words
3. Microsoft Excel

3.4 Design and Fabricate Models.

Considering the fact that the project involves designing and fabricating aspect of Savonius rotor and test rig of partially bounded flow and fully bounded flow, the design constraints have to be identified prior to the designing of the model. The design constraints are identified as below:

3.4.1 Design Constraints

a. Weight Issues

- The weight of the model shall not be too heavy as it will affect the installation process, and causes difficulties when assembling and dismantling of Savonius rotor from the test rig.
- Weight of the materials and dimensioning shall be taken into considerations when designing the Savonius rotor model and test rig.

b. The Ease of Formability of Material

- The design of rotor and test rig will involve curvature; hence the formability of the material shall be taken into considerations when choosing the material.
- Materials such as steels or aluminium sheets are taken into consideration when designing the Savonius rotor blades.

c. Height Issues

- Since the experiment will be conducted in block 18, the height of the final assembly will be taken into consideration in order for the model to fit comfortably and ease of working.

d. The Stability of The Model

- The model shall be assembled and supported properly when conducting the experiment. Steel frame shall be used, to construct and erect the model in a standing position in order to utilize the wind output from the wind tunnel.

3.4.2 Design Criteria

In order to ensure proper designing of the Savonius Rotor, research and data collection through literature review is conducted. However there are no available standards from any association or bodies in the design of Savonius Rotor, hence the design criteria are selected based on logic and analysis. The design criteria that are determined to be important to the project are as below:

- The end plate, D_r of the design should be 10% larger than the rotor diameter. [4, 11]
- A two step rotor is found to be producing the best efficiency. [11]
- The aspect ratio meaning the height, h over the diameter of rotor, D of 2 seems to lead to the best power coefficient. However, not all the designs in the literature review follow suit the proposed aspect ratio. And in the case of this project and aspect ratio of 1 is used in order to standardize three different rotor designs. [4,11]
- A primary overlapping, e between the rotors is found to be best around $0.15d$ - $0.30d$. (d = rotor diameter). [4]

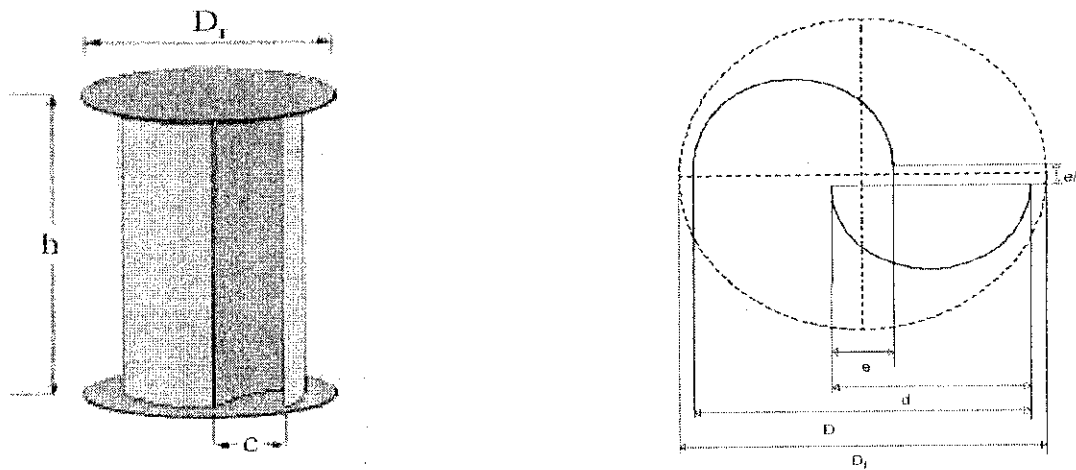


Figure 3.1: Schematic Dimension of Two Bladed Rotors. ^{Ref[4]}

3.4.3 Material Selection

Table 3.1: Pugh Selection Matrix for End Plate's Material.

Design criterion \ Materials	Criterion Weightage	Perspex	Metal Plate
Weight	0.40	5	3
Availability	0.15	5	5
Easiness of Fabrication	0.30	4	4
Cost	0.15	5	3
Total	1.00	4.70	3.60

Table 3.2: Pugh Selection Matrix for Rotor Blade's Material.

Design criterion \ Materials	Criterion Weightage	Steel Sheet	Aluminium Sheet
Weight	0.40	4	5
Availability	0.15	5	5
Easiness of Fabrication	0.30	5	5
Cost	0.15	4	4
Total	1.00	4.50	4.75

Scale:-

4-5 above acceptance range

3 within acceptance range

1-2 below acceptance range

By referring to the Pugh Selection Matrix, Table 3, Perspex is the optimum material that can be used for fabrication of end plates. Reason being Perspex is lighter in weight, easily available, lower in cost and relatively easy in fabrication process. Metal plates can be use as well; however the factor of weight issues omitted its usability and the cost would be relatively higher.

For the selection of rotor blades material, aluminium sheets will be chosen instead for the fabrication. Reason being, the materials are available in the manufacturing laboratory. Apart from that, aluminium sheets are relatively lighter as compared to steel sheets.

3.4.4 Dimension Analysis

In order to design three different Savonius Rotor design. Dimensional analysis should be made before moving on to the drawing of the designs. The design criteria mentioned prior to this will be taken into account as well. Before making the dimensional analysis, there will be some predetermined dimensions such as height and diameter size of the rotor. The height and diameter of the rotor are taken to be 30cm.

a) Rotor 1

By referring to Figure 3.1, given the total blade diameter, D equals to 30 cm and the height of the blade equals to be 30 cm, hence the end plate size should be 10% larger of total blade diameter which is equals to 33cm and the rotor diameter, d is 17.5.

Hence, the primary overlapping, e should be,

$$e = 17.5 * 2 - 30 = 5$$

b) Rotor 2

By referring to Figure 2.3, ϕ is found through literature review to be the best at a range of $124^{\circ} - 135^{\circ}$ [5]. Hence, through discussion a decision is made to have ϕ of 130° in the design. Having to standardize the end plate size to 33cm and through literature review [5] m which are known as the offset are taken to

be 4.5cm. While the primary overlap, e are taken to be 2.25cm. In order to calculate the radius of the arc, r and the straight section of the blade, p, and the calculations are as follow.

$$15 \sin 40 = r - \frac{m}{2} + r \sin 40 \quad (1)$$

$$9.6 = 1.64r - \frac{m}{2} \quad (2)$$

Through literature review [5], given $\frac{m}{D} = 0.15$, $m = 4.5$ since $D=30$, putting $m=4.5$ into (2) we get $r=7.23\text{cm}$. Through literature review [5],

$$\frac{p}{r} = 0.2 \quad (3)$$

Is found to produce the best efficiency, by putting $r=7.23\text{cm}$ into (3) we get $p= 1.45\text{cm}$.

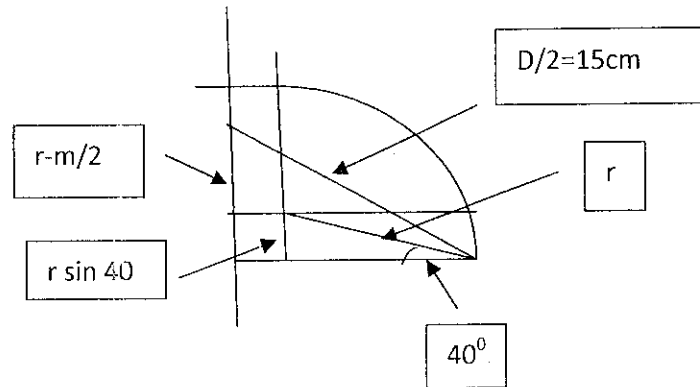


Figure 3.2: Dimensional Analysis of Blade Design 2.

However, with the consideration of reducing or minimize the wind flow or escape from the side or tip of the blade, the rotor blade dimension of r and p is increases to 9cm and 1.8cm. It is found through trial and error method to while drawing using AutoCAD software that, the propose dimension is appropriate to be use.

c) Rotor 3

By referring to Figure 18, given $d=2\text{cm}$, height = 60 cm and length of rotor blade equals to 13 and a small curvature with radius 1.5cm at an angle 90° .

By putting the dimension into (1) we get $r=14\text{ cm}$.

$$\frac{d}{2} + r = 15 \quad (1)$$

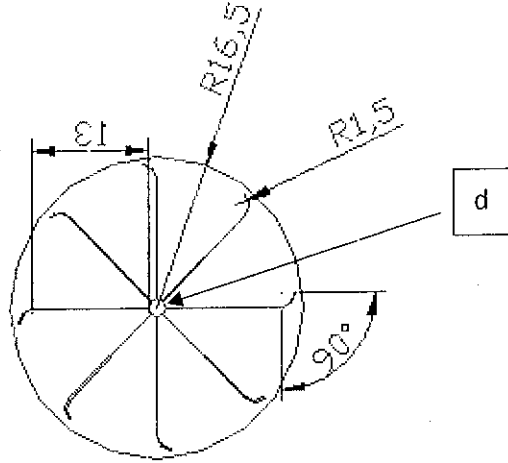


Figure 3.3: Top View of Design 3.

Each blade is given a length, l of 11cm, with a total of eight blades, the total offset, s between each blade is,

$$60.4 = (8 * l) - 7s$$

And the offset, s equals to 3.94cm.

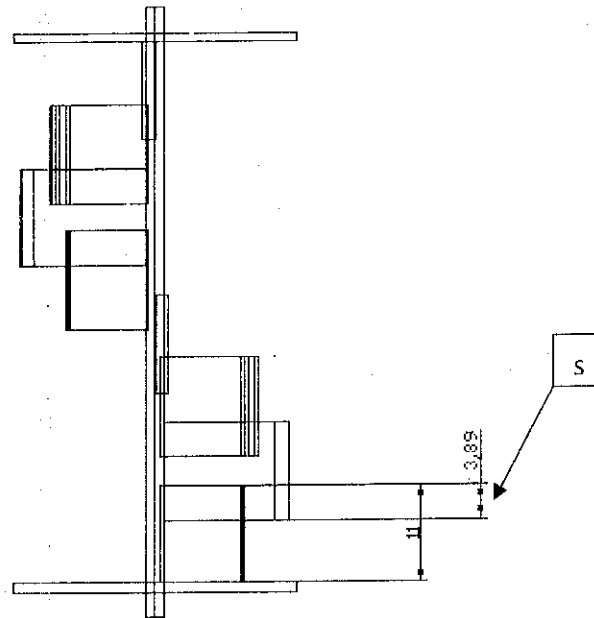


Figure 3.4: Side View of Design 3.

3.4.5 Prototype Design

The different rotor design and test rig design for partially bounded and fully bounded flow will be displayed in 3D, top view and side view together with the dimensions in the appendix section.

3.4.6 Fabrication of Rotor

The end plates are made by external fabricator doing precision cutting to prepare the slots for slotting of blades. The shafts are designed and fabricated in such a way that the base of the shafts can be glued to the end plates and a 4cm protruding shaft through the center with 1cm in diameter for rotor design 1 and design 2. For design 3, a shaft of 68cm long with 1cm in diameter is fabricated. A stopper plate with the dimension of 33cm in diameter and a center hole of 1cm and 2mm thick is designed and fabricated; the reason is to prevent the blades from slotting pass the end plates. The blades are made by aluminum sheet with 1mm thickness; the sheets are cut into desired widths which are 47.12cm for rotor 1, 14.65cm for rotor 2 both with a length of 30cm. For rotor 3 8 smaller blades are cut with 11 cm in length and a width

of 15.36cm. The assemblies of the rotors are made by gluing the parts together using Ebstik Glue, as well as super glue to increase strength of hold. The total height is standardized for all rotors, which is 628mm.

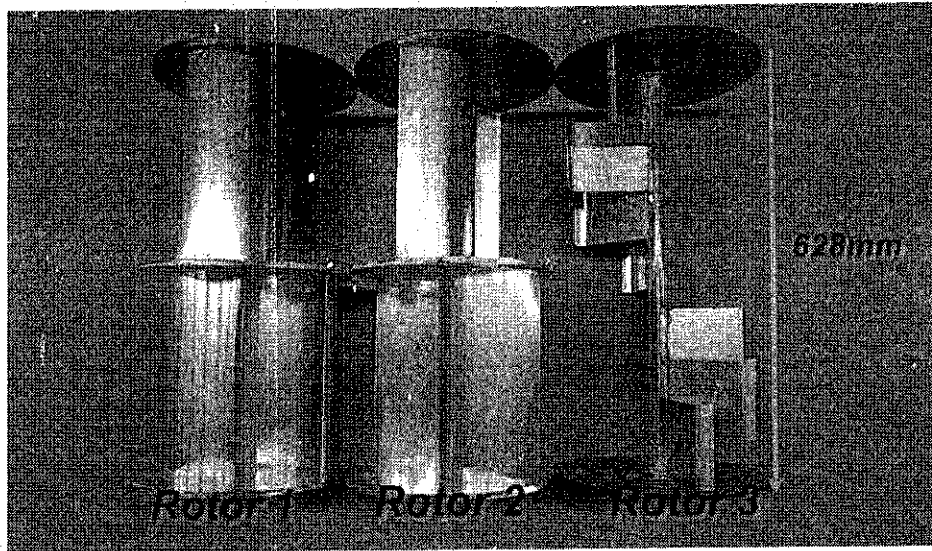


Figure 3.5: From Left to Right Prototype Rotor 1, 2 and 3

The rotor shafts are attached with 10mm size low friction bearings, to allow rotational movement for the rotor when attached to the bush on the test rig.

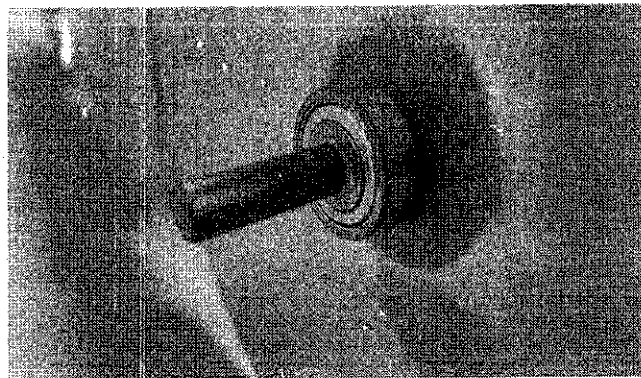


Figure 3.6: Attachment of Low Friction Bearing to Rotor Shaft

3.5 Design and Fabricate Experimental Test Rig.

3.5.1 Test Rig Design

Experimental test rigs are an important element in this research work, the main purpose of the test rigs is to direct the flow to the rotors install within the rig and to reduce the wind loses comparing to unbounded operation of wind rotor. Two test rigs are design and fabricated for this experiment,

namely partially bounded casing and fully bounded casing. For partially bounded casing, the inlet of the wind is larger and wind is allowed to hit on both the concave and convex side of the blades. For fully bounded casing, the wind inlet is smaller the convex side of the blade is sealed off to allow only the concave blades to be hit by the wind. The detailed design of the test rigs can be viewed from the Appendix section. Below are the 3D figures of partially bounded and fully bounded casings.

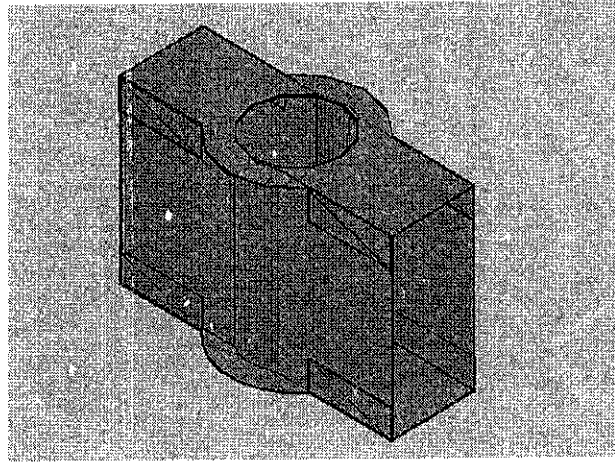


Figure 3.7: Partially Bounded Casing

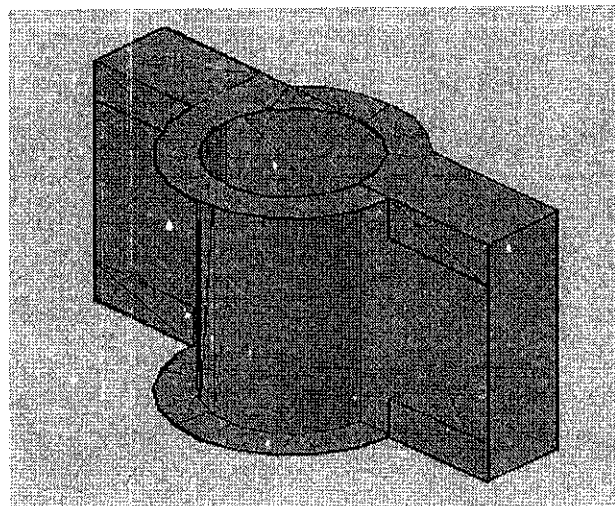


Figure 3.8: Fully Bounded Casing

3.5.2 Material Selection

Table 3.3: Pugh Selection Matrix for Test Rig material

Design criterion \ Materials	Criterion Weightage	Mild Steel Plate	Aluminium Plate
Weight	0.40	4	5
Availability	0.15	5	5
Easiness of Fabrication	0.30	5	3
Cost	0.15	5	3
Total	1.00	4.75	4.00

Steel plate has been chosen for the usage of fabricating the test rig, reason being that steel plate is relatively cheaper in cost and ease of fabricating purposes, comparing to aluminium plate, mild steel plates can be welded more easily. Despite that the casing make from mild steel plate would be slightly heavier as compared to aluminium plate, the weight can actually help to stabilize the experimental fixtures, if the rotors rotating at high speeds.

3.5.3 Fabrication of Test Rig

The fabrication work is done by external fabricator who has the expertise in doing bending, rolling and welding work. The end product is painted to avoid abrasion as well as for aesthetic purpose. The figure below showed the fabricated test rigs.

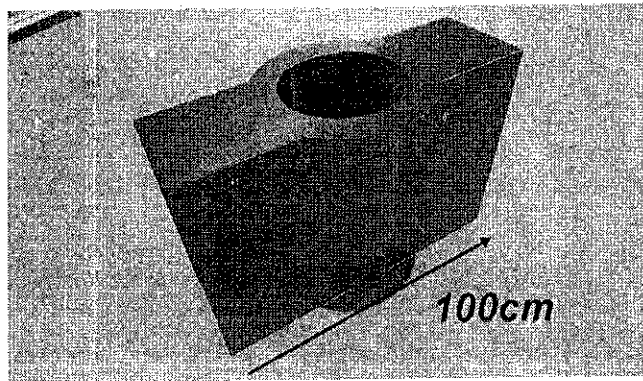


Figure 3.9: Fabricated Partially Bounded Casing

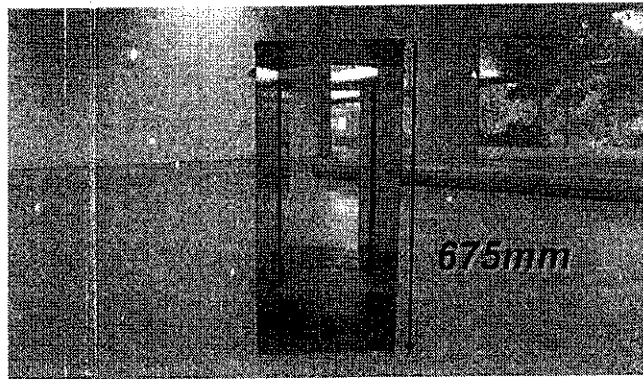


Figure 3.10: Front View of Fabricated Partially Bounded Casing

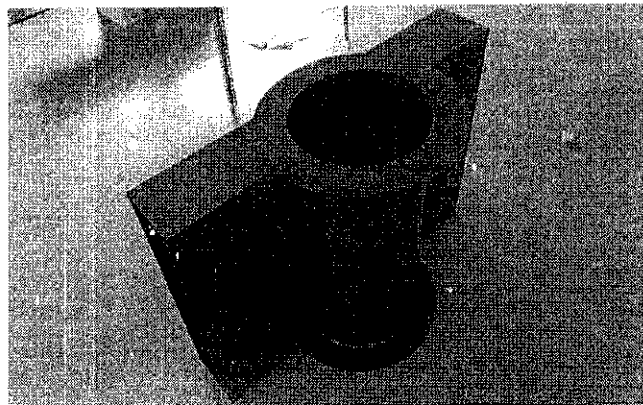


Figure 3.11: Fabricated Fully Bounded Casing

3.6 Experimental Procedure

The set up of the experiment is shown in the figure below:

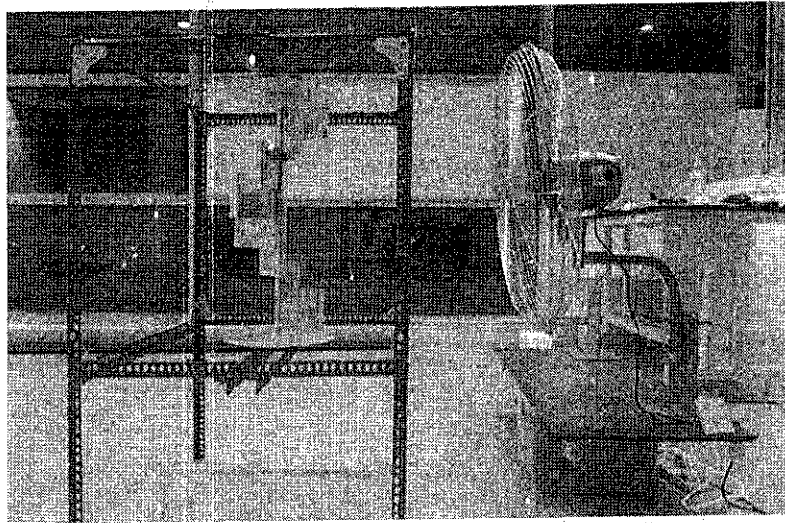


Figure 3.12: Experiment Set Up

For the experiment, an industrial fan with 70cm in diameter is used as the wind source. The fixture is made from pivoted angle bars standing at 112 cm tall, 80 cm width and 80 cm in length. The rotors are held by a specially design bush at both ends and is fixed to the fixture using steel girders by bolts and nuts. The wind source is placed as closed to the fixtures as possible to reduce loses of strength in the wind source, the distance between the fixture to the fan is approximately 30cm, reason being for the tolerance is due to allocation for the 1 meter in length casing later on when placed onto the fixture. A dimmer switch is fixed to the industrial fan to regulate the desire wind speed for the experiment.

For the experiment, three different rotors are fabricated namely rotor 1, 2 and 3. All three rotors will be tested in different environment, namely, open environment, partially bounded environment and fully bounded environment where the test rigs will come into play. A wind speed of 1m/s to 7m/s is desired and is achieved by regulating the dimmer switch attached to the industrial fan. The wind speed will be measured by using a vane anemometer at 3 different spots namely top, middle and bottom closest to the fixtures, due to the nature of the wind from the industrial fan, the wind speed will not be constant at all spots, instead an average will be taken, a tolerance of ± 0.2 m/s is acceptable for the wind average.

The rotational speed, ω in RPM, of the rotor resulting from the wind speed will be measured by a digital tachometer. A reflective strip is stick at the top plate of the rotor, and the measurement is taken by pointing the laser tip of the tachometer onto the reflective strip. Measurement will only be taken when the turning of the rotor stabilizes, three different readings will be taken each time, and the average will be considered.

The torque, T in N.m, produce by the rotor due to the wind speed is measured using a torque meter by clamping it to the shafts. Since the torque is fluctuating due to the turning of rotor, the maximum will be taken and three measurements will be taken and the average will be considered.

Each rotor will complete open environment, partially bounded environment, and fully bounded environment testing. The results will be recorded and tabulated in Microsoft Excel.

3.7 Flow Chart

Below are the Work Flow Chart throughout the design, fabrication and experimental stages of the project

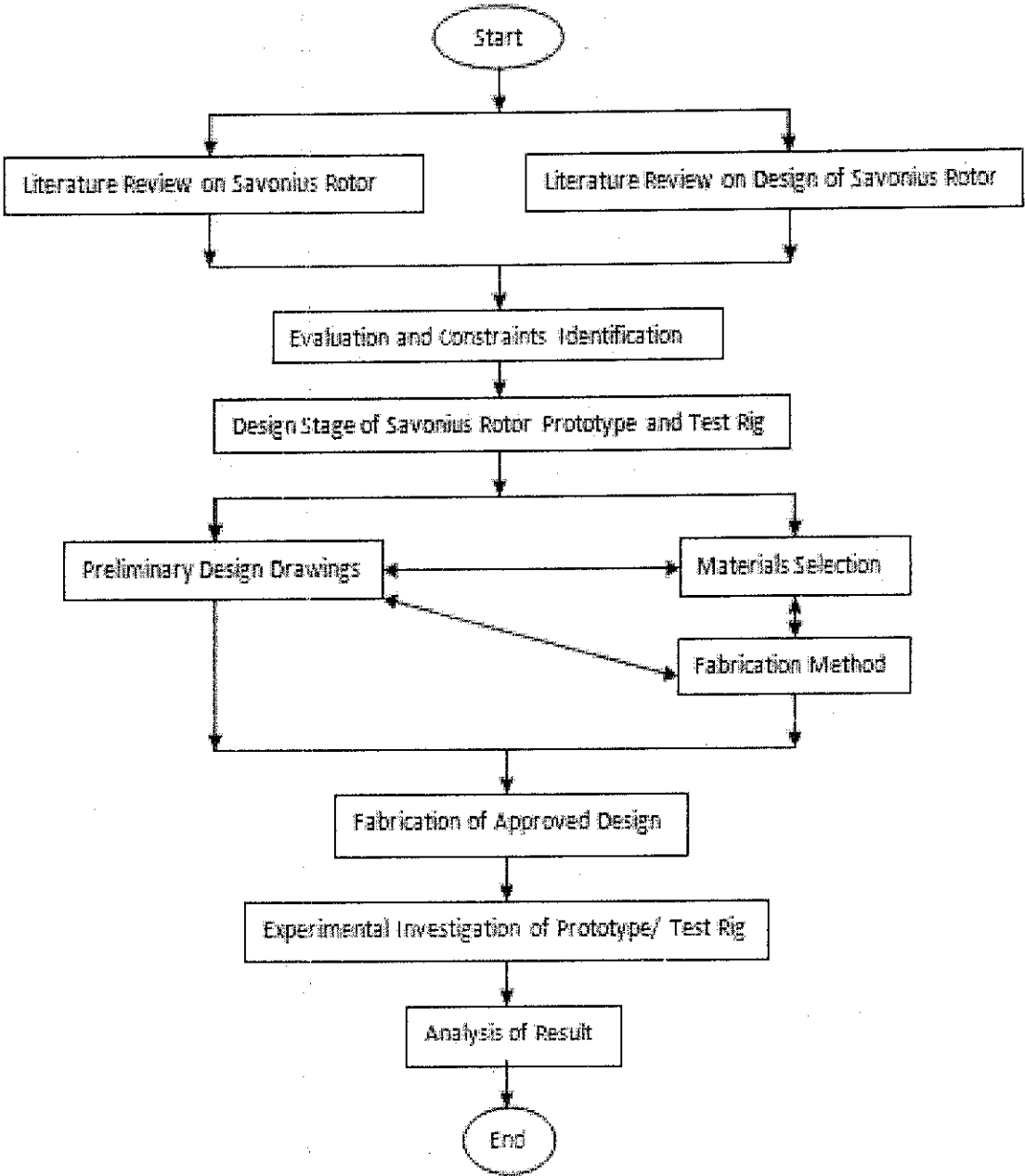
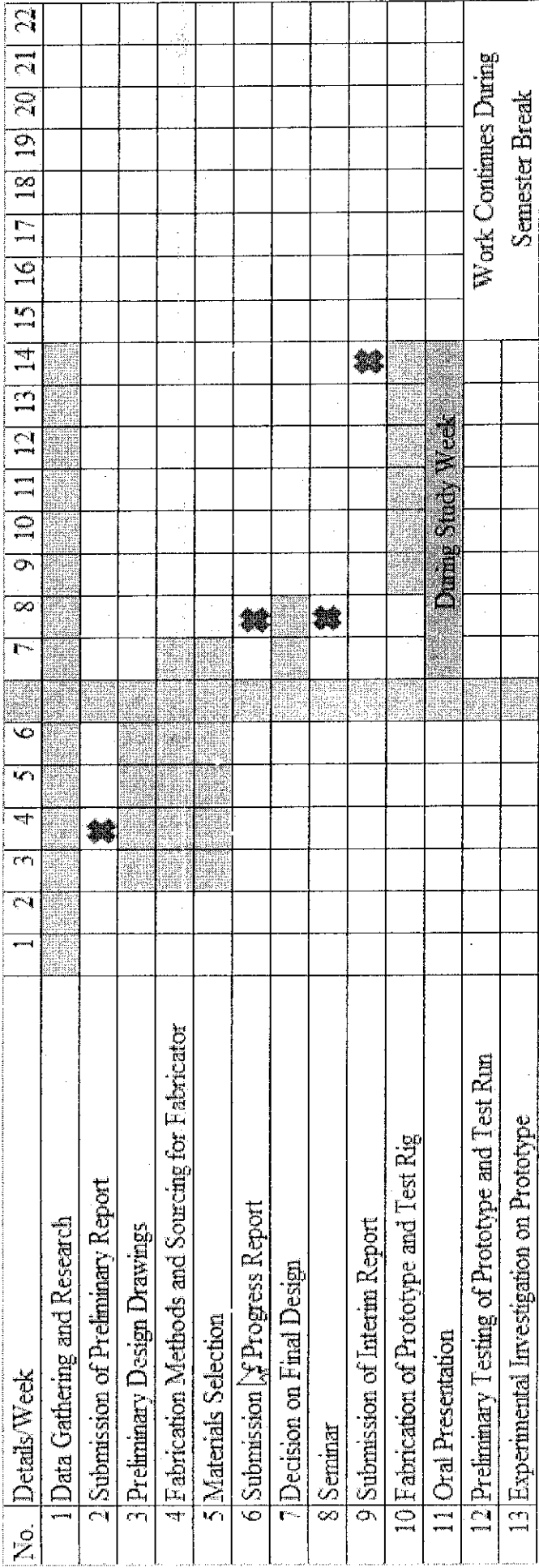


Figure 3.13: Flow Chart for Final Year Project.

3.8 Gantt Chart

3.8.1 Final Year Project 1



✿ Key Milestones

Figure 3.14: Gantt chart for Final Year Project 1

3.8.2 Final Year Project 2

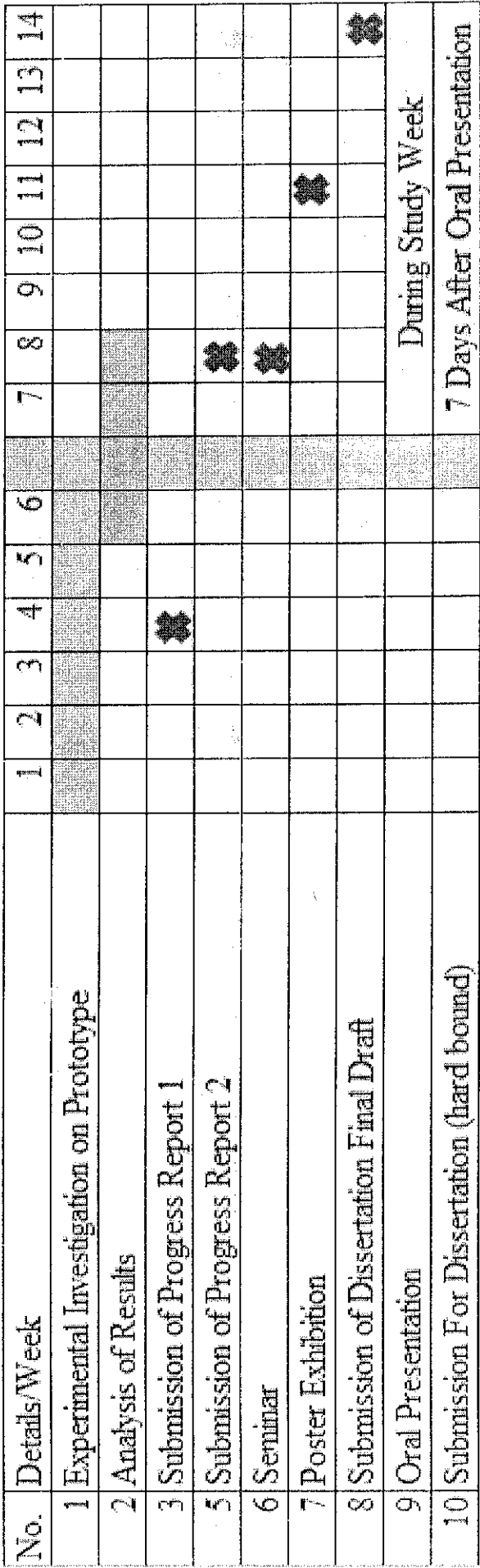


Figure 3.15: Gantt chart for Final Year Project 2

CHAPTER 4

RESULT AND DISCUSSION

4.1 DATA GATHERING AND ANALYSIS

The experiment has been conducted under standard room conditions, with 1atm pressure, and approximately 26-27⁰C room temperature. The results are gathered based on the experiment of three different rotors operating at open, partially bounded and fully bounded environment at wind velocity ranging from 1m/s to 7m/s. The objective is to determine the power coefficient , C_p and torque coefficient C_T of the rotors. The results are analyzed and are compared between different operating conditions as well as the performance between each other. The formulas involved in calculations are as below:

- Wind Power, $P_w = \frac{1}{2}\rho V^3 A_{\text{rotor}}$
- Tip Speed Ratio (TSR), $\lambda = (\omega.r) / V$
- Rotor rotational speed, $\omega = 2\pi N / 60$
- Rotor Power, $P_{\text{rotor}} = \omega.T$
- Torque (T), N.m measured using torque meter.
- Power coefficient , $C_p = P_{\text{rotor}} / P_w$
- Torque Coefficient, $C_T = T / (1/2 \rho V^3 A_{\text{rotor}}(D/2))$

Table 4.1: Data for Wind Speed, Rotor Rotational Speed and Torque in Open Environment

No.	Wind Speed (V), m/s	Rotor 1		Rotor 2		Rotor 3	
		Rotational Speed, ω RPM	Torque (T), N.m	Rotational Speed, ω RPM	Torque (U), N.m	Rotational Speed, ω RPM	Torque (T), N.m
1	1.00	0.00	0.005670	0.00	0.002000	0.00	0.002000
2	2.00	80.27	0.038000	0.00	0.005330	0.00	0.006000
3	3.00	176.27	0.068330	0.00	0.029000	37.80	0.009000
4	4.00	265.00	0.083000	60.27	0.088000	65.87	0.017670
5	5.00	361.37	0.120670	103.77	0.105670	77.37	0.036000
6	6.00	409.03	0.143300	123.57	0.116000	114.20	0.074000
7	7.00	531.60	0.234000	149.17	0.138000	120.67	0.110300

Table 4.2: Data for Wind Speed, Rotor Rotational Speed, Torque in Partially Bounded Environment

No.	Wind Speed (V), m/s	Rotor 1		Rotor 2		Rotor 3	
		Rotational Speed, w RPM	Torque (T), N.m	Rotational Speed, w RPM	Torque (T), N.m	Rotational Speed, w RPM	Torque (T), N.m
1	1.00	0.00	0.007330	0.00	0.003330	0.00	0.003000
2	2.00	98.93	0.041000	6.00	0.006670	18.60	0.006000
3	3.00	194.53	0.077000	0.00	0.033670	35.20	0.020667
4	4.00	274.10	0.112000	72.60	0.082333	57.97	0.038330
5	5.00	353.37	0.144670	94.20	0.139330	76.60	0.057700
6	6.00	374.03	0.165333	103.97	0.150000	90.50	0.077333
7	7.00	425.47	0.248700	133.97	0.196670	103.93	0.099667

Table 4.3: Data for Wind Speed, Rotor Rotational Speed, Torque in Fully Bounded Environment

No.	Wind Speed (V), m/s	Rotor 1		Rotor 2		Rotor 3	
		Rotational Speed, ω RPM	Torque (T), N.m	Rotational Speed, ω RPM	Torque (T), N.m	Rotational Speed, ω RPM	Torque (T), N.m
1	1.00	0.00	0.007310	0.00	0.005300	0.00	0.002000
2	2.00	82.17	0.009400	0.00	0.014330	27.00	0.004333
3	3.00	232.00	0.014330	0.00	0.018333	59.90	0.008670
4	4.00	315.93	0.044000	84.17	0.027000	106.13	0.012000
5	5.00	336.50	0.075000	177.40	0.042670	134.13	0.026700
6	6.00	398.20	0.120000	199.47	0.073670	162.43	0.041330
7	7.00	467.77	0.144700	238.67	0.121330	182.23	0.053670

Table 4.4: Results for Rotor 1, 2 and 3 in Open Environment

	TSR, λ	Wind Power, P, watt	Rotor Power, Protor, watt	Power coefficient, C_p	Torque Coefficient, C_t
Rotor 1	0.0000	0.1113	0.0000	0.0000	0.3397
	0.6305	0.8901	0.3193	0.3587	0.2846
	0.9231	3.0041	1.2607	0.4196	0.1516
	1.0408	7.1209	2.3021	0.3233	0.0777
	1.1354	13.9080	4.5641	0.3282	0.0578
	1.0710	24.0330	6.1349	0.2553	0.0398
	1.1931	38.1636	13.0199	0.3412	0.0409
Rotor 2	0.0000	0.1113	0.0000	0.0000	0.1198
	0.0000	0.8901	0.0000	0.0000	0.0399
	0.0000	3.0041	0.0000	0.0000	0.0644
	0.2367	7.1209	0.5551	0.0780	0.0824
	0.3260	13.9080	1.1477	0.0825	0.0507
	0.3235	24.0330	1.5003	0.0624	0.0322
	0.3348	38.1636	2.1546	0.0565	0.0241
Rotor 3	0.0000	0.1113	0.0000	0.0000	0.1198
	0.0000	0.8901	0.0000	0.0000	0.0449
	0.1979	3.0041	0.0356	0.0119	0.0200
	0.2587	7.1209	0.1218	0.0171	0.0165
	0.2431	13.9080	0.2915	0.0210	0.0173
	0.2990	24.0330	0.8845	0.0368	0.0205
	0.2708	38.1636	1.3931	0.0365	0.0193

Table 4.5: Results for Rotor 1, 2 and 3 in Partially Bounded Environment

	TSR, λ	Wind Power, P, watt	Rotor Power, Protor, watt	Power coefficient, C_p	Torque Coefficient, C_t
Rotor 1	0.0000	0.1113	0.0000	0.0000	0.4392
	0.7771	0.8901	0.4245	0.4770	0.3071
	1.0187	3.0041	1.5678	0.5219	0.1709
	1.0765	7.1209	3.2132	0.4512	0.1049
	1.1103	13.9080	5.3508	0.3847	0.0693
	0.9793	24.0330	6.4725	0.2693	0.0459
	0.9549	38.1636	11.0752	0.2902	0.0434
Rotor 2	0.0000	0.1113	0.0000	0.0000	0.1995
	0.0000	0.8901	0.0000	0.0000	0.0500
	0.0000	3.0041	0.0000	0.0000	0.0747
	0.2851	7.1209	0.6256	0.0879	0.0771
	0.2960	13.9080	1.3737	0.0988	0.0668
	0.2722	24.0330	1.6323	0.0679	0.0416
	0.3007	38.1636	2.7577	0.0723	0.0344
Rotor 3	0.0000	0.1113	0.0000	0.0000	0.1798
	0.1461	0.8901	0.0117	0.0131	0.0449
	0.1843	3.0041	0.0761	0.0253	0.0459
	0.2277	7.1209	0.2326	0.0327	0.0359
	0.2407	13.9080	0.4626	0.0333	0.0277
	0.2370	24.0330	0.7325	0.0305	0.0215
	0.2332	38.1636	1.0842	0.0284	0.0174

Table 4.6: Results for Rotor 1, 2 and 3 in Fully Bounded Environment

	TSR, λ	Wind Power, P, watt	Rotor Power, Protor, watt	Power coefficient , Cp	Torque Coefficient, Ct
Rotor 1	0.0000	0.0556	0.0000	0.0000	0.8760
	0.6454	0.4451	0.0808	0.1816	0.1408
	1.2149	1.5021	0.3480	0.2317	0.0636
	1.2408	3.5604	1.4550	0.4086	0.0824
	1.0573	6.9540	2.6415	0.3799	0.0719
	1.0426	12.0165	5.0014	0.4162	0.0666
	1.0498	19.0818	7.0845	0.3713	0.0506
Rotor 2	0.0000	0.0556	0.0000	0.0000	0.6351
	0.0000	0.4451	0.0000	0.0000	0.2147
	0.0000	1.5021	0.0000	0.0000	0.0814
	0.3306	3.5604	0.2379	0.0668	0.0506
	0.5574	6.9540	0.7923	0.1139	0.0409
	0.5223	12.0165	1.5381	0.1280	0.0409
	0.5356	19.0818	3.0309	0.1588	0.0424
Rotor 3	0.0000	0.0556	0.0000	0.0000	0.2397
	0.2121	0.4451	0.0122	0.0275	0.0649
	0.3137	1.5021	0.0544	0.0362	0.0385
	0.4168	3.5604	0.1333	0.0374	0.0225
	0.4214	6.9540	0.3748	0.0539	0.0256
	0.4253	12.0165	0.7027	0.0585	0.0229
	0.4090	19.0818	1.0237	0.0536	0.0188

4.2 RESULTS AND DISCUSSION

4.2.1 Comparison between Rotors

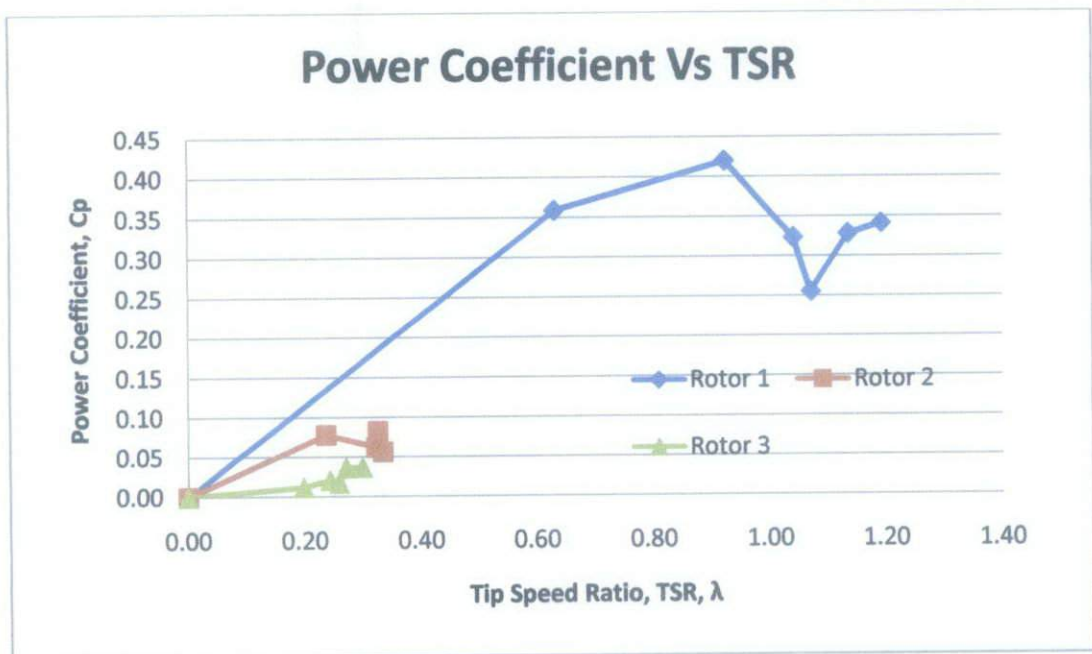


Figure 4.1: The Power coefficient versus TSR for Rotors

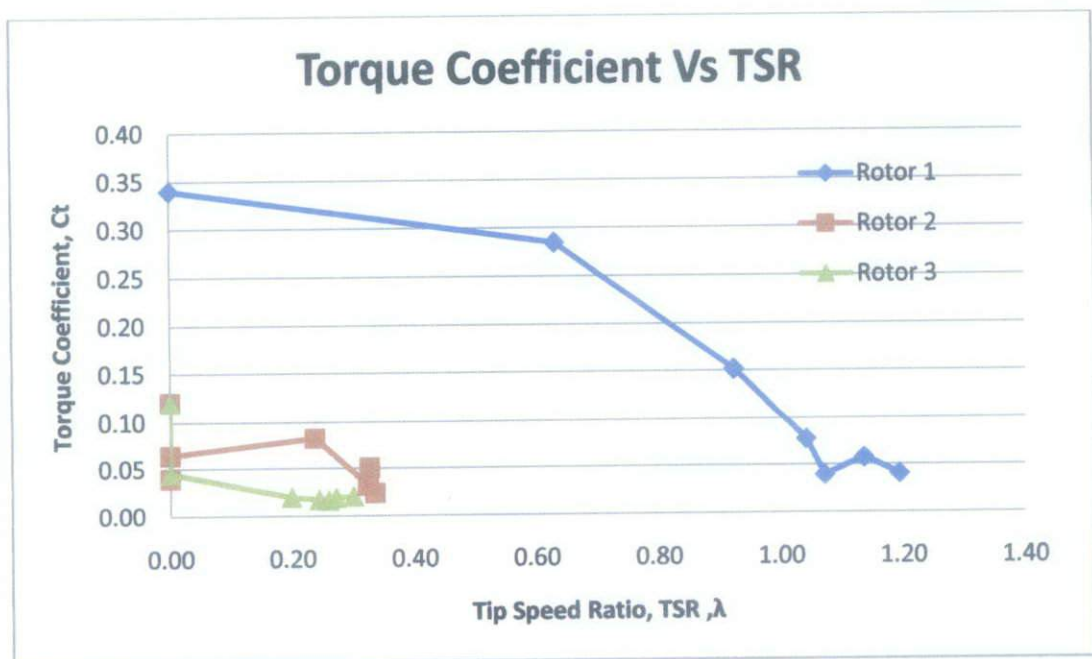


Figure 4.2: The Torque Coefficient versus TSR of Rotors

Figure 4.1 above shows the result of power coefficient versus tip speed ratio, TSR for Rotor 1, 2 and 3. The maximum power coefficient for Rotor 1 is 0.4196 at TSR of 0.9231. For Rotor 2, the maximum power coefficient is 0.0825 at TSR of 0.3260.

Lastly for Rotor 3, the maximum coefficient is 0.0368 occurs at TSR of 0.2990. From the results shown above, it can be clearly determine that Rotor 1 has the best power coefficient followed by Rotor 2 and Rotor 3.

Under figure 4.2, maximum torque for Rotor 1, 2 and 3 happens at TSR equals to zero, the maximum torque for Rotor 1 is 0.3397 and for Rotor 2 and 3 both is 0.1198. The torque decreases as TSR increases, from the graph Rotor 1 has better torque coefficient compare to Rotor 2 and Rotor 3. R

As we can see, Rotor 1 performs much better as compared to Rotor 2 and 3. There are several factors that contribute to the low performance of Rotor 2 and 3. The main contributor would be the rotor designs, unlike Rotor 1, Rotor 2 curves from the tip and has a straight at end, and the design allows wind to pass through when hitting the concave blade without follow up to push the second blade. For rotor 3, the curvature at the tip might not be enough to capture the wind, unlike Rotor 1 and 2; it has much smaller radius at the curvature and longer straights at the end. Other causes could be due to weight, abrasion in bearings and assembly mistake.

4.2.2 Comparison between Operating Environments for Rotor 1

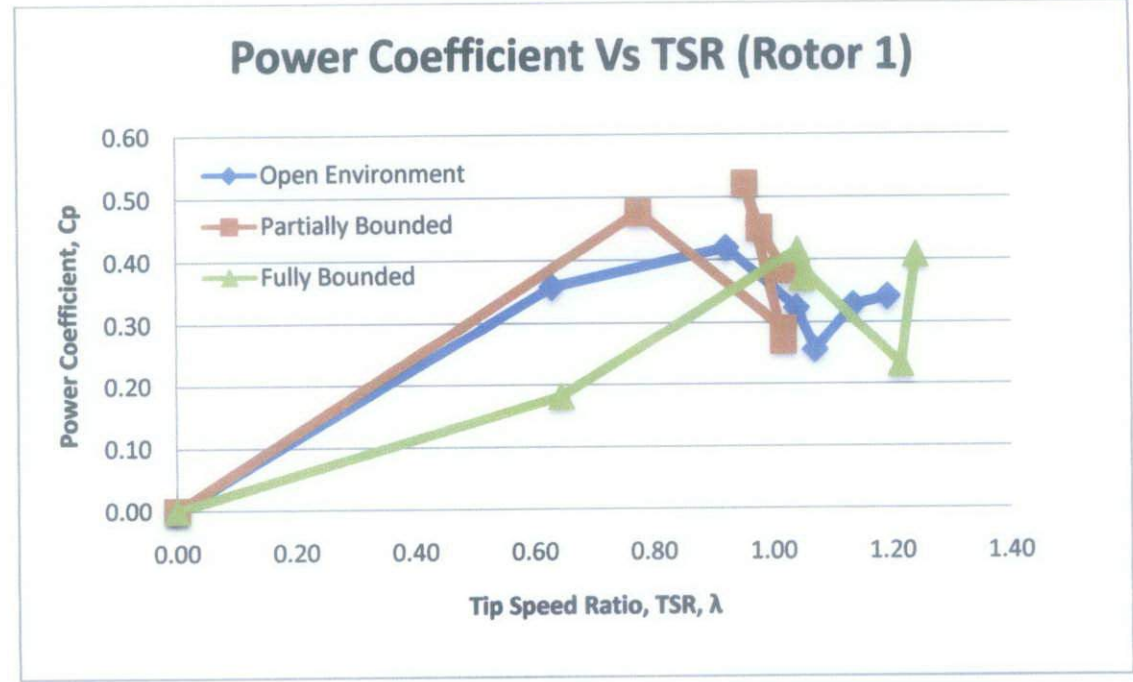


Figure 4.3: C_p Comparison between Operating Environments of Rotor 1

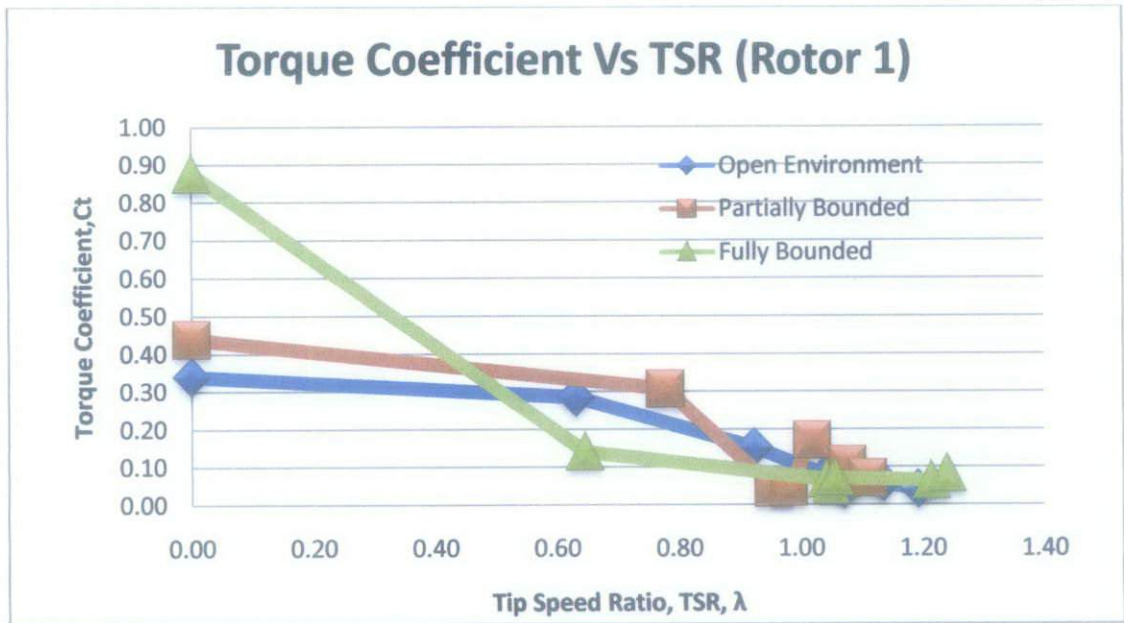


Figure 4.4: C_T Comparison between Operating Environments of Rotor 1

From Figure 4.3, Rotor 1 achieves the highest power coefficient at partially bounded environment, with a C_p of 0.5219 at TSR of 1.0187. Follow suit is operation in open environment with a C_p of 0.4196 at TSR of 0.9231. Lastly is operation in fully bounded environment with a C_p of 0.4162 at TSR of 1.0426. In general the C_p increases in bounded flow operations for Rotor 1, highest C_p is achieved at a range of TSR from 0.8-1.2.

Figure 4.4 shows the Torque Coefficient for Rotor 1 in different operating environments. The maximum Torque Coefficient is achieved when TSR is equals to zero. The maximum Torque Coefficient is achieved by operating Rotor 1 in fully bounded environment where C_T equals to 0.8760. For operation in partially bounded environment C_T is 0.4392 and lastly for open environment is 0.3397. If comparing TSR at a range from 0.60-1.20, operation in partially bounded flow is much better comparing to fully bounded and open environment.

As we can see from figure 4.3 and 4.4, operation in fully bounded casing does not performs as predicted, however Rotor 1 appears to be operating better at partially bounded environment, and C_p is much higher comparing to other operating environments and C_T appears to be higher comparing to fully bounded casing when Rotor 1 operated at TSR from 0.60-1.20. The reason for lower performance in fully bounded casing might due to the smaller opening of wind inlet as compare to partially bounded casing, certain amount of wind from the fan might be blocked.

However do note that for fully bounded casing, Rotor 1 is capable in operating at higher TSR.

4.2.3 Comparison between Operating Environment for Rotor 2

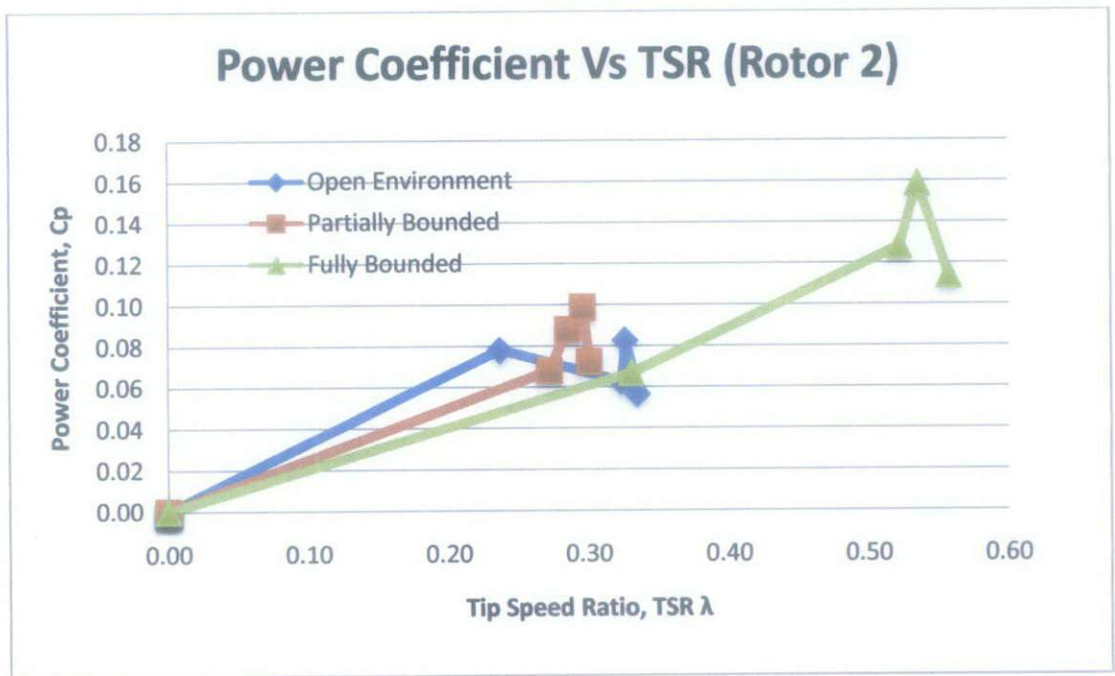


Figure 4.5: C_p Comparison between Operating Environments of Rotor 2

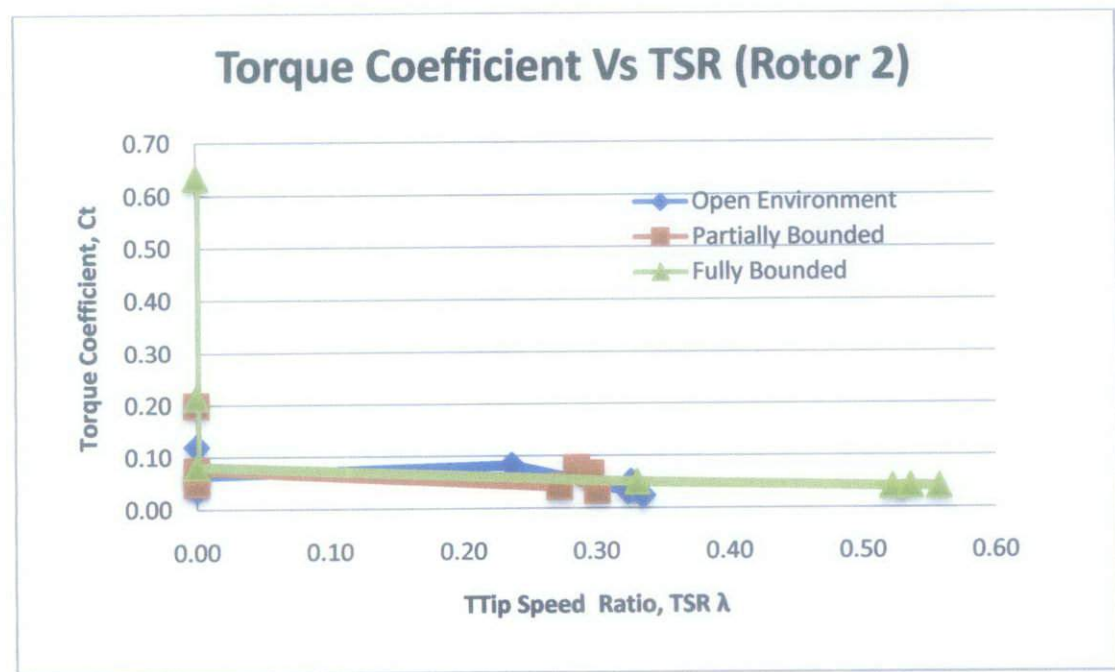


Figure 4.6: C_t Comparison between Operating Environments of Rotor 2.

Figure 4.5 shows the comparison of C_p between different operating environments for Rotor 2. For Rotor 2, the maximum power coefficient is achieved by operating in

fully bounded environment, where C_p equals to 0.1588 at TSR of 0.5356. The maximum C_p for partially bounded environment is 0.0988 at TSR of 0.2960. Lastly the maximum C_p for open environment is 0.0825 at TSR of 0.3260. With the use of fully bounded casing Rotor 2 is able to achieve higher TSR and C_p . In general the use of casing in Rotor 2 increases the C_p of Rotor 2.

On Figure 4.6 is the Torque Coefficient comparison between operating environments for Rotor 2. Maximum C_T is 0.6351 at TSR of 0 in fully bounded environment. The torque coefficient then decreases with the increase in TSR. For open environment, the maximum C_T is 0.1198 when TSR is zero. The maximum torque for partially bounded environment is 0.1995 when TSR is zero. Fully bounded environment is better when TSR is zero to achieve higher torque coefficient, however when operated at a TSR range of 0.20-0.35, open environment and partially bounded environment has better C_T , 0.0824 and 0.0771 each. However, for fully bounded operation, Rotor 2 is capable in achieving higher TSR and torque coefficient.

4.2.4 Comparison between Operating Environments for Rotor 3

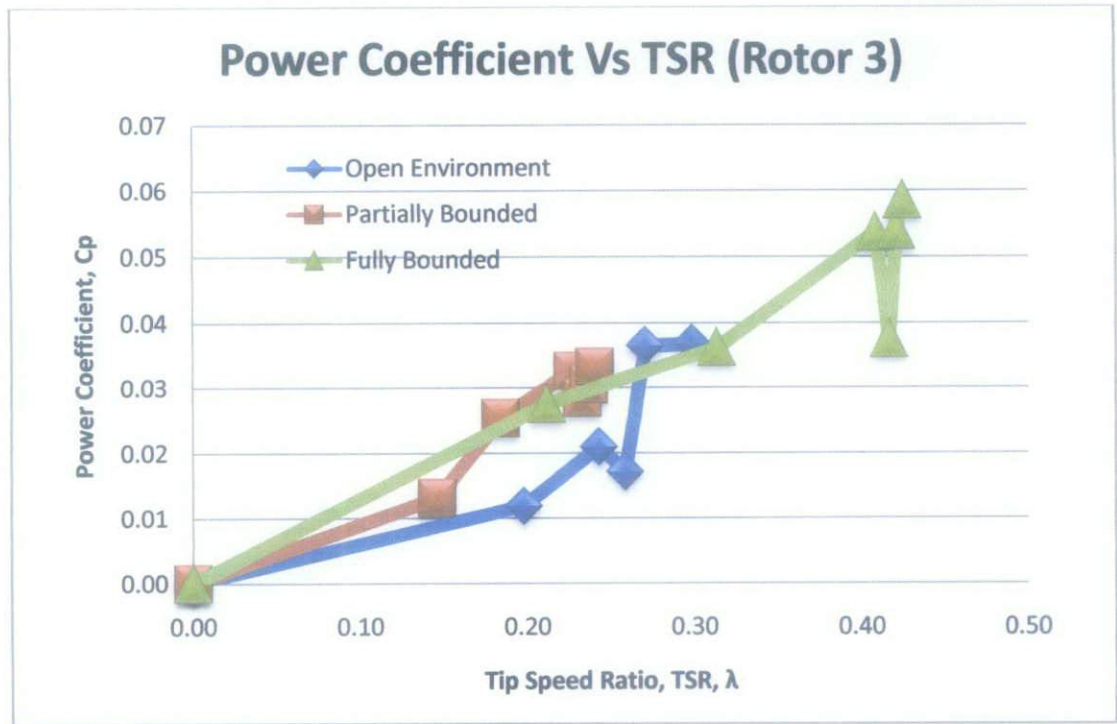


Figure 4.7: C_p Comparison between Operating Environments for Rotor 3

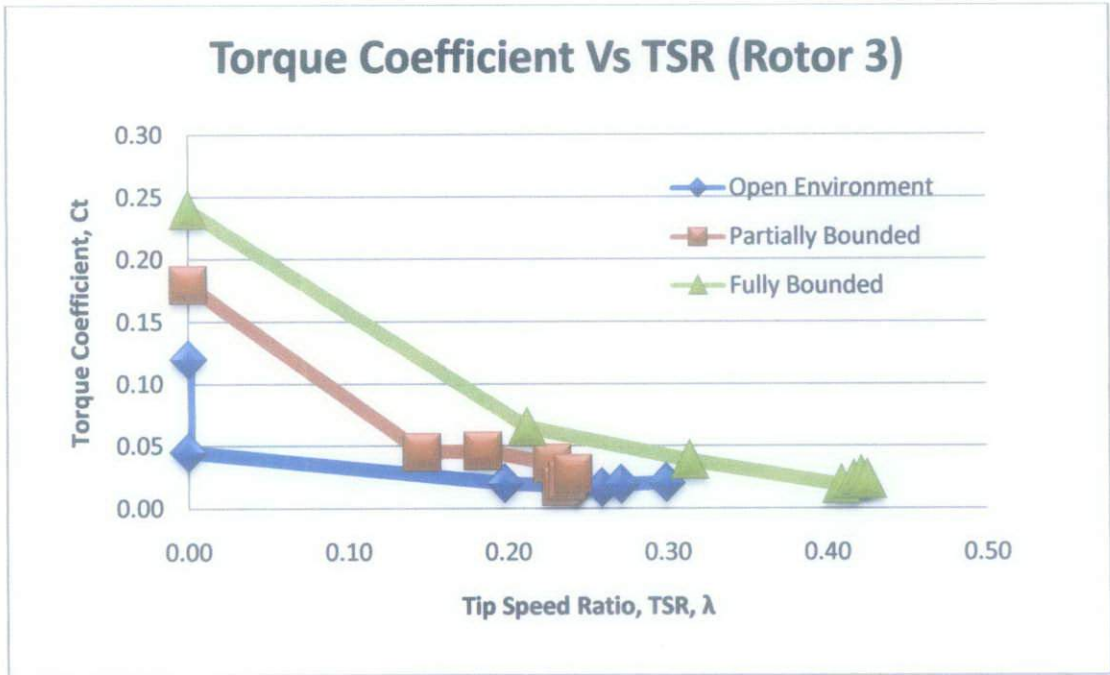


Figure 4.8: C_T Comparison between Operating Environment for Rotor 3

From figure 4.7, the maximum C_p for Rotor 3 is 0.0585 at TSR of 0.4253 operating under fully bounded environment. For open environment, the maximum C_p is 0.0368 at TSR of 0.2990. Under operation of partially bounded environment the maximum C_p is 0.0333 at TSR of 0.2407. With the operation of fully bounded environment, Rotor 3 is capable of achieving higher C_p at higher TSR. If compare the range of TSR between 0-0.25, it can be seen that under operation in partially bounded environment the C_p increases as compared to open environment.

Figure 4.8 shows the C_T comparison between operating environments for Rotor 3. Highest C_T is 0.2397 at TSR of zero for fully bounded environment. For partially bounded environment maximum C_T is 0.1798 at TSR of zero. Lastly for open environment maximum C_T is 0.1198 at TSR of zero. With operation in fully bounded environment, higher C_T can be achieved, as well as higher TSR.

CHAPTER 5

CONCLUSION & RECOMMENDATION

5.1 CONCLUSION

The project has given the exposure and understanding of the design of Savonius wind rotors as well as the operating characteristics. The experimental work is carried out successfully in this project. Three different rotors namely rotor 1, 2 and 3 is fabricated based on research and discussion with supervisor. Rotor 1 utilizes the conventional rotor design, while rotor 2 is modified Savonius rotor with a straight end and curve tip; the dimension is based on literature review and dimension analysis. Rotor 3 is a newly design wind rotor with no reference available so far. All three rotors are compared between each other and compared between different operating environments. The conclusions drawn from the experiment are as below:

1. Improve Starting Capabilities

The starting capabilities of Rotors improve with operation in bounded environment. For operation in open environment, Rotor 1 start turning at 2.7m/s without any need of torque to start, while Rotor 2 starts turning at approximately 4m/s, Rotor 3 starts turning at approximately 3m/s. Under the operation of partially bounded environment, Rotor 1 starts turning at 1.7m/s and Rotor 2 starts at 3.4m/s, lastly Rotor 3 is capable to start at approximately 2m/s. For fully bounded environment, Rotor 1 starts at approximately 2m/s and Rotor 2 starts approximately 3.4m/s, lastly Rotor 3 manage to start at 1.8m/s.

2. Improve power coefficient , C_p

In general, there is enhancement in C_p for all Rotors when operated in bounded environment as compared to open environment. With the operation in bounded environment, Rotors are capable in achieving higher TSR as compared to open environment. Rotor 1 achieved maximum C_p under partially bounded operation, while Rotor 2 and 3 achieved better C_p when operated in fully bounded environment.

3. Improve Torque Coefficient, C_T

In general higher C_T is achieved when operating in bounded environment. For Rotor 1, highest C_T is achieved when operated in partially bounded environment, for Rotor 2 and 3; highest C_T is achieved when operated in fully bounded environment.

From the results of the experiment, it is possible to conclude that the performance of Rotors can be enhanced with the operation in bounded environment.

5.2 RECOMMENDATION

Few important points have been noted when conducting the project in order to better improve the project as well as for further research work to be conducted and is divided into parts, they are:

1. Prototype design and fabrication

During the design of prototype, weight shall be taken into account when making decisions on the thickness on end plates, thickness of the blades and shafts. Select light weight material and proper thickness to provide just enough rigidity to the prototype and not overly thick and contribute to weight gain. Choose thin, light materials for fabrication of blades, despite using 1mm aluminium sheets, there is still some difficulties when moulding the blades into desire shapes, recommended thickness would be around 0.8mm. Since a two steps rotor is required, during fabrication, ensure proper alignment of the rotor and the 90 degrees difference in angle between two rotors, request for assistance when doing the fabrication work.

2. Casing design and fabrication

During the design of the casing, despite having smaller tolerance between the inserting holes and the rotor is better, having a slightly larger tolerance is better to ensure easiness in assembly later on. Ensure light weight material is used for the fabrication of casing, to ease assembly for experiment later on. Since the manufacturing lab does not possess the necessary tools and skills required to do the work, outside manufacturer has to be source, ensure that the work done by external fabricator is proper and follow according to the specifications given.

3. Improvement in Experimental Work

The current experimental work is done using an industrial fan as the wind source and the wind speed is regulated by a regulator from 1m/s-7m/s. The maximum wind speed from the industrial fan is 7m/s, it is recommended to run the experiment using a wind tunnel with a better range of wind speed up to 15m/s. The reason that wind tunnel is not being used, is due to the downtime of wind tunnel, over heating on the motor and the long waiting list. Always repeat the experiment at least three times to ensure the consistency of result obtained.

More research work can be done on the experiment of Savonius rotor. Some recommendations are, improve the wind speed range to for better understanding of the operating characteristics of the three prototypes that are designed. Improvement on the designs of Rotor 3 with difference in blade curvature can be done through simulation or experimental work. Apart from that, generator can be implemented on the current experimental work to investigate possible electricity output that can be produced by the three rotors.

REFERENCES

- [1] http://en.wikipedia.org/wiki/Wind_turbine. Date 15 August 2010
- [2] http://www.ask.com/wiki/Savonius_wind_turbine. Date 15 August 2010
- [3] M.H. Mohamed, G. Janiga, E. Pap, D. Thévenin; 2010, “Optimization of Savonius Turbines Using an Obstacle Shielding the Returning Blade”, Germany, Renewable Energy, 35, 2618-2626.
- [4] U.K. Saha a, S. Thotla a, D. Maity b; 2008, “Optimum design configuration of Savonius rotor through wind tunnel experiments”, India, Journal of Wind Engineering and Industrial Aerodynamics, 96, 1359- 1375.
- [5] M.A. Kamoji a, S.B. Kedare a, S.V. Prabhu b, 2009, “Experimental investigations on single stage modified Savonius rotor”, India, Applied Energy, 86, 1064–1073.
- [6] Modi VJ, Fernando MSUK, 1989; “On the performance of the Savonius wind turbine”. JSol Energy Eng, 111:71–81.
- [7] Burçin Deda Altan *, Mehmet Atılğan, 2008, “An experimental and numerical study on the improvement of the performance of Savonius wind rotor”, Turkey, Energy Conversion and Management, 49, 3425–3432.
- [8] Kunio Irabu, Jitendro Nath Roy, 2007, “Characteristics of wind power on Savonius rotor using a guide-box tunnel”, Japan, Experimental Thermal and Fluid Science, 32, 580–586.
- [9] M.H. Mohamed, G. Janiga, E. Pap, D. Thévenin , 2010 , “Optimal blade shape of a modified Savonius turbine using an obstacle shielding the returning blade”, Germany, Energy Conversion and Management xxx, xxx–xxx.

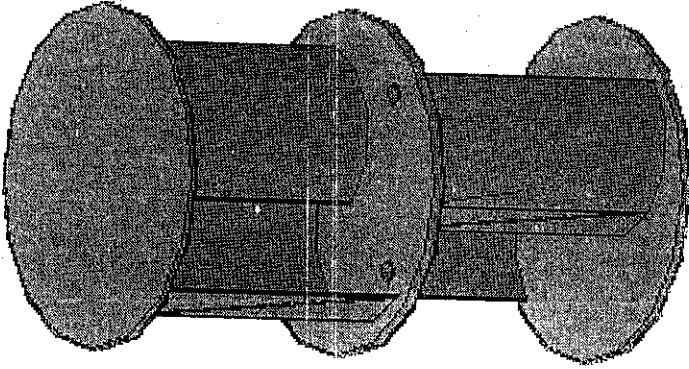
[10] A. S. Grinspan, P. Suresh Kumar, U. K. Saha, P. Mahanta, D. V. Ratna Rao and G. Veda Bhanu, “ Design, Development and Testing of Savonius Wind Turbine with Twisted Blades”.

[11] Jean-Luc Menet¹, Nachida Bourabaa², “Increase in The Savonius Rotor Efficiency via Parametric Investigation”, France.

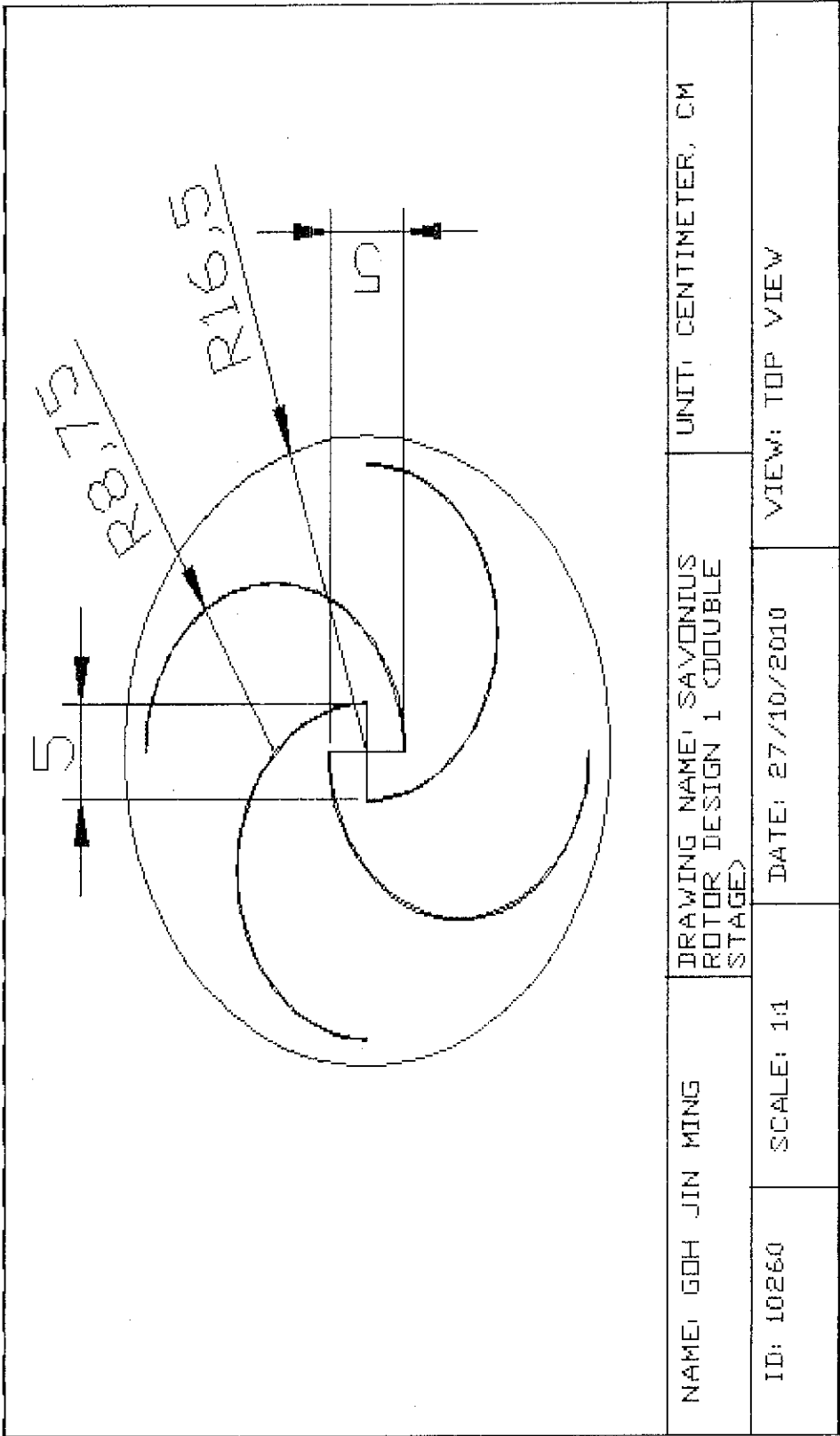
APPENDICES

APPENDIX 1:	Design 1 3D
APPENDIX 2:	Design 1 Top View
APPENDIX 3:	Design 1 Side View
APPENDIX 4:	Design 1 Middle Top View
APPENDIX 5:	Design 2 3D
APPENDIX 6:	Design 2 Top View
APPENDIX 7:	Design 2 Side View
APPENDIX 8:	Design 2 Middle Top View
APPENDIX 9:	Design 3 3D
APPENDIX 10:	Design 3 Top View
APPENDIX 11:	Design 3 Side View
APPENDIX 12:	Partially Bounded Test Rig 3D
APPENDIX 13:	Partially Bounded Test Rig Top View
APPENDIX 14:	Partially Bounded Test Rig Side View
APPENDIX 15:	Fully Bounded Test Rig 3D
APPENDIX 16:	Fully Bounded Test Rig Top View
APPENDIX 17:	Fully Bounded Test Rig Side View

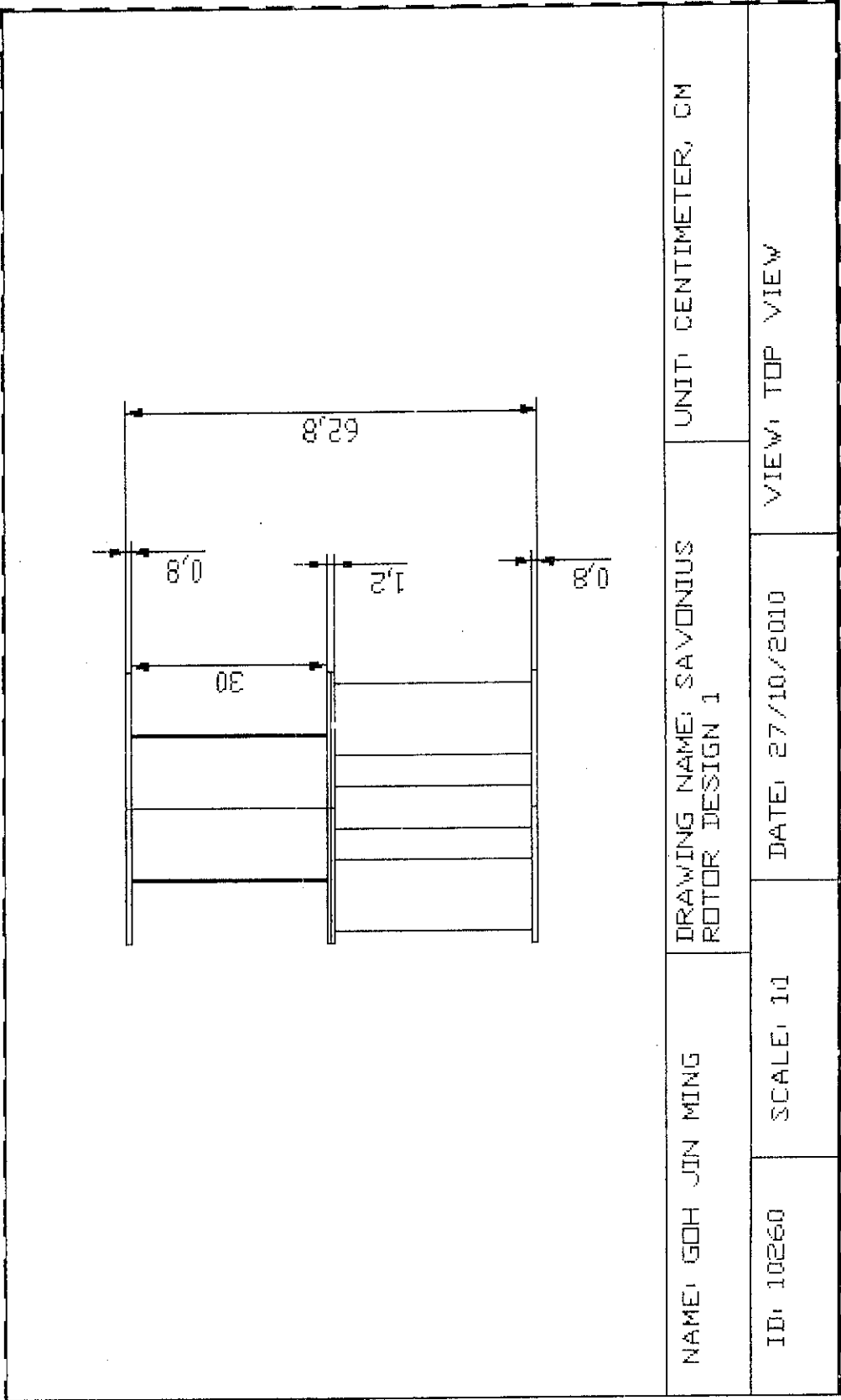
NAME: GOH JUN KING		DRAWING NAME: SAVONIUS ROTOR DESIGN 1 DOUBLE STAGE		UNIT: CENTIMETER, CM
ID: 10260	SCALE: 1:1	DATE: 27/10/2010	VIEW: 3D VIEW	



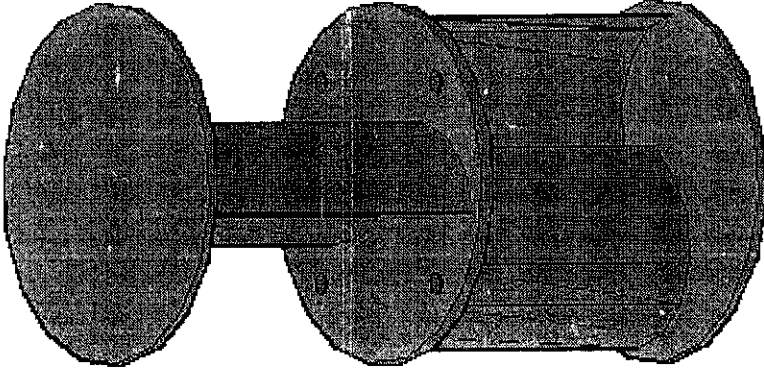
APPENDIX 1: Savonius Rotor Design 1 3D



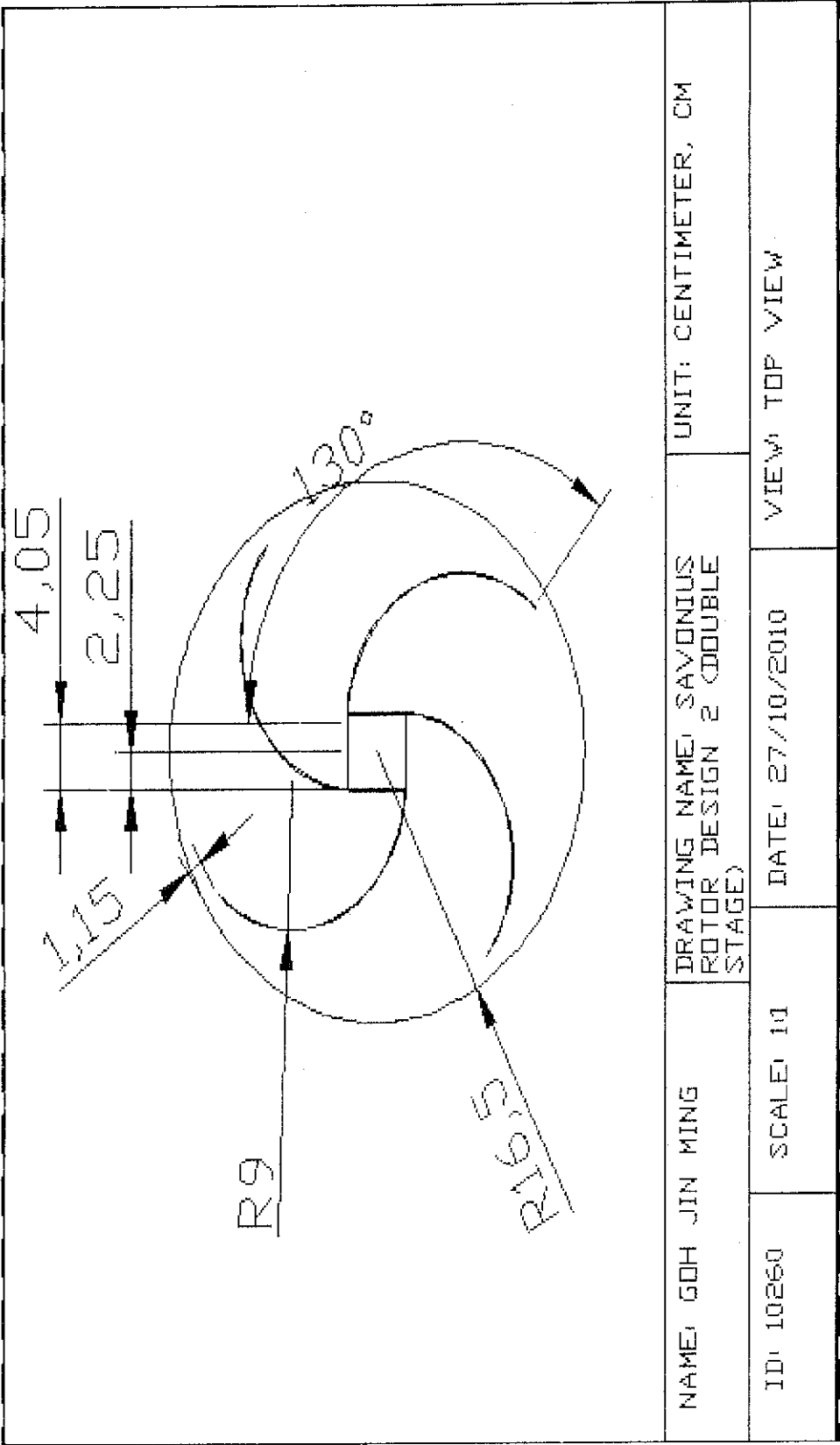
APPENDIX 2: Savonius Rotor Design 1 Top View



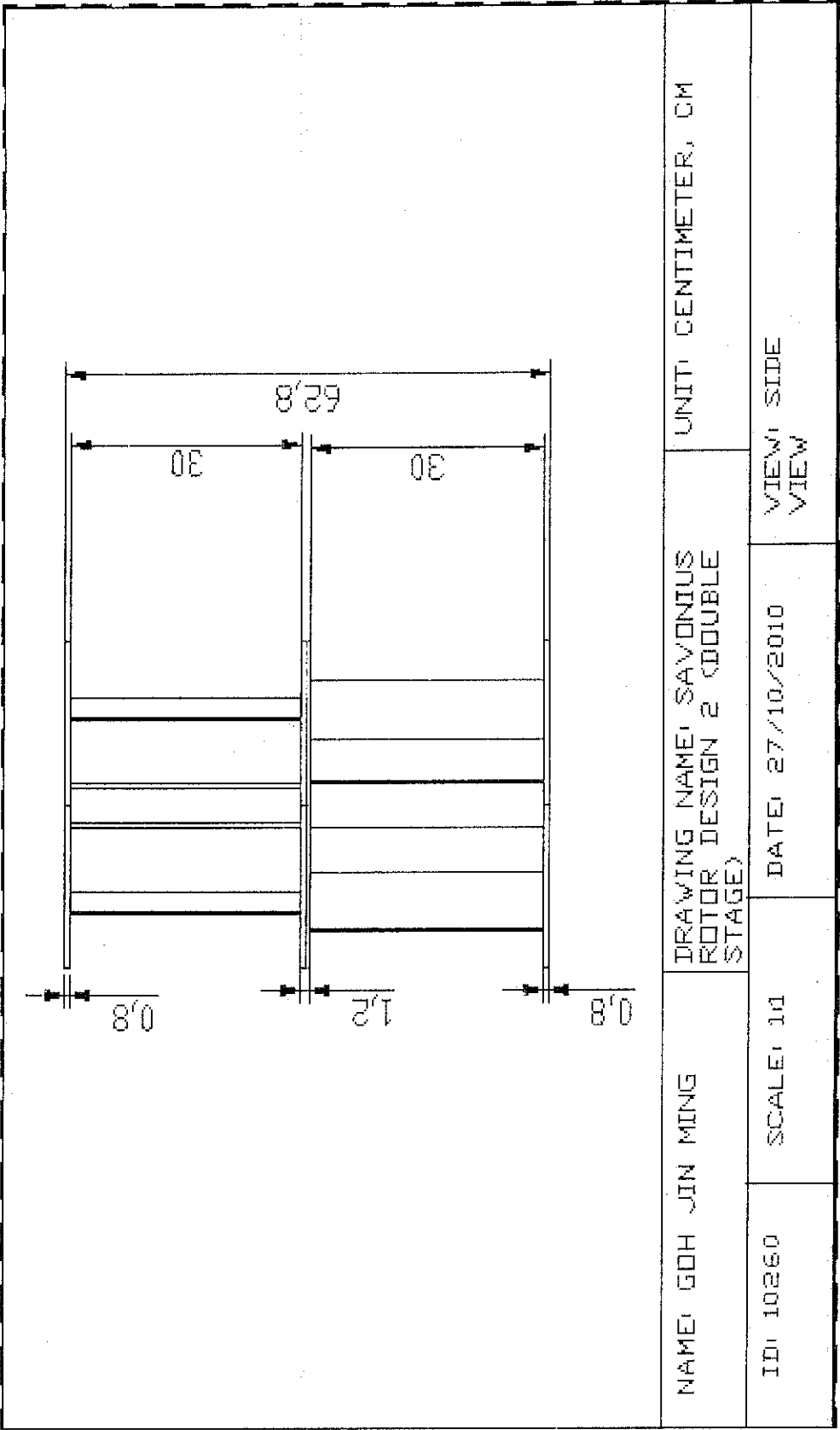
APPENDIX 3: Savonius Rotor Design 1 Side View

				UNIT: CENTIMETER, CM
NAME: GOH JIN MING		DRAWING NAME: SAVONIUS ROTOR DESIGN 2 (DOUBLE STAGE)		
ID: 10260	SCALE: 1:1	DATE: 27/10/2010	VIEW: 3D VIEW	

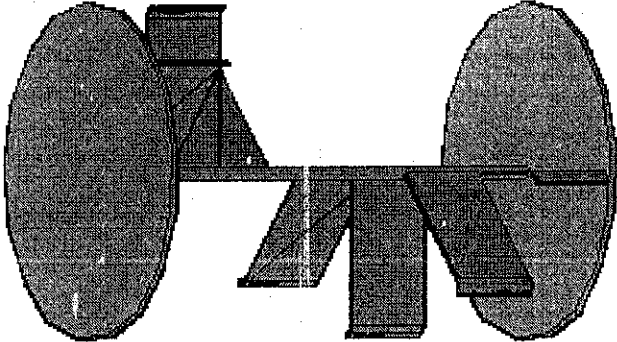
APPENDIX 4: Savonius Rotor Design 2 3D View



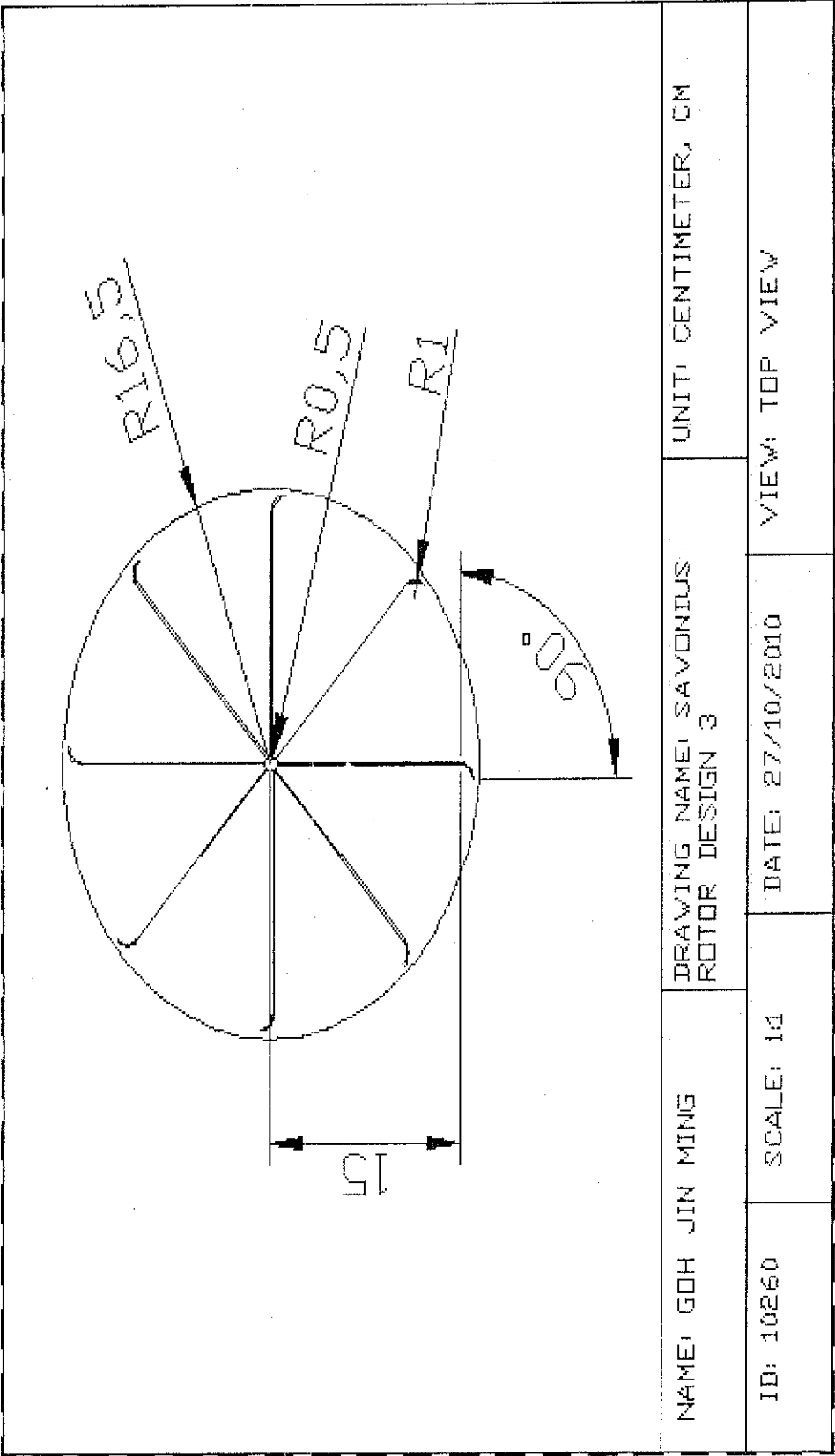
APPENDIX 5: Savonius Rotor Design 2 Top View



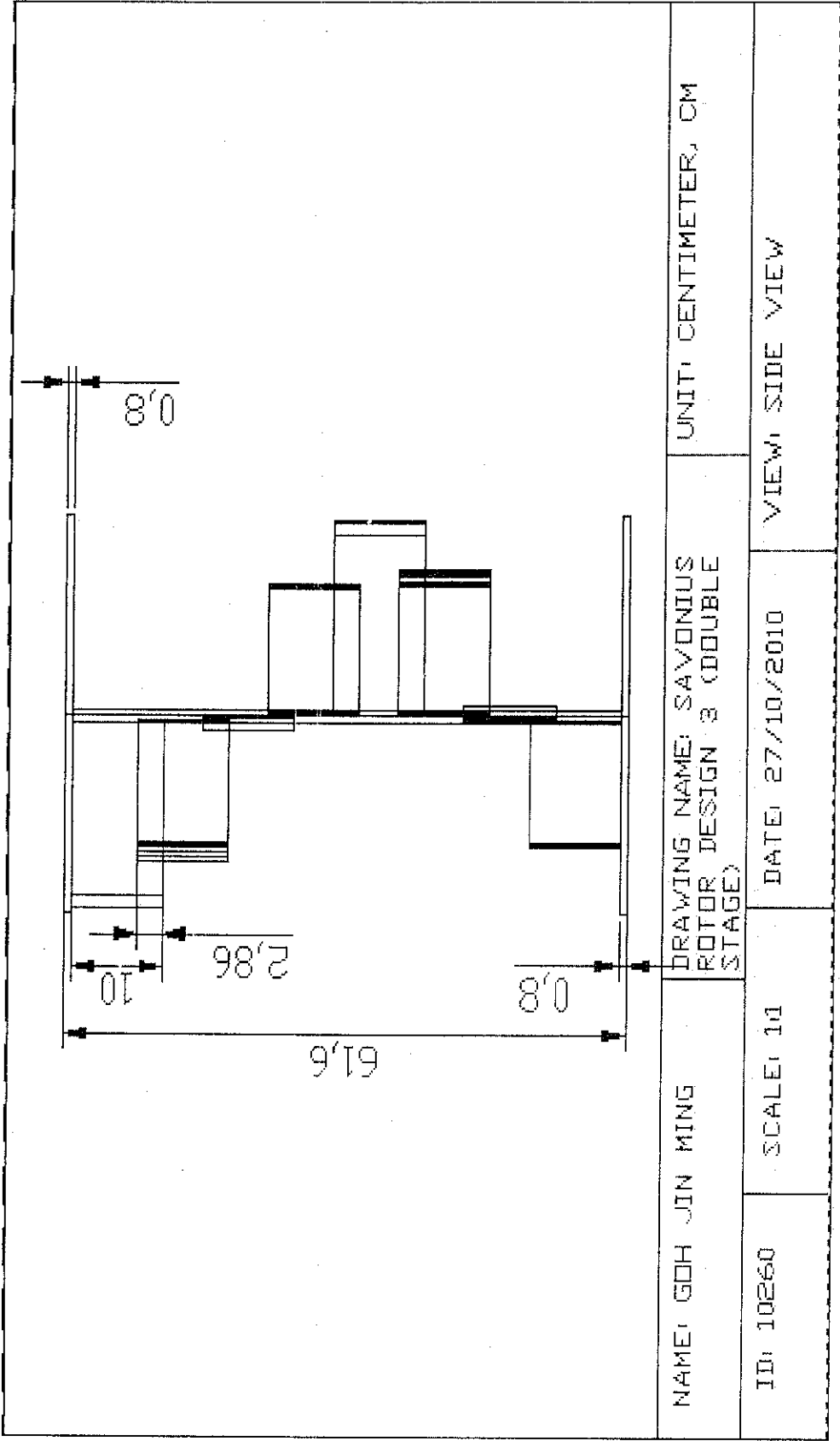
APPENDIX 6: Savonius Rotor Design 2 Side View

				UNIT: CENTIMETER, CM	
NAME: GOH JIN MING		DRAWING NAME: SAVONIUS ROTOR DESIGN 3 (DOUBLE STAGE)		VIEW: 3D	
ID: 10260	SCALE: 1:1	DATE: 27/10/2010			

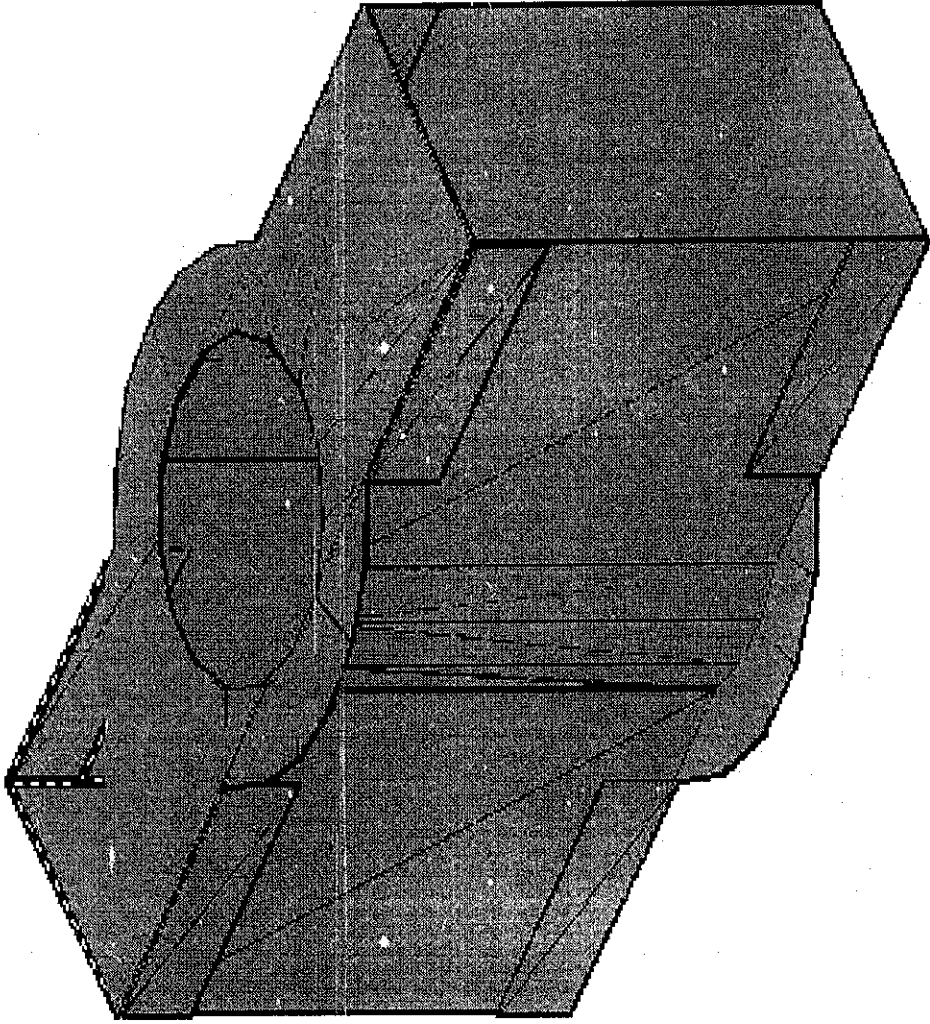
APPENDIX 7: Savonius Rotor Design 3 3D View



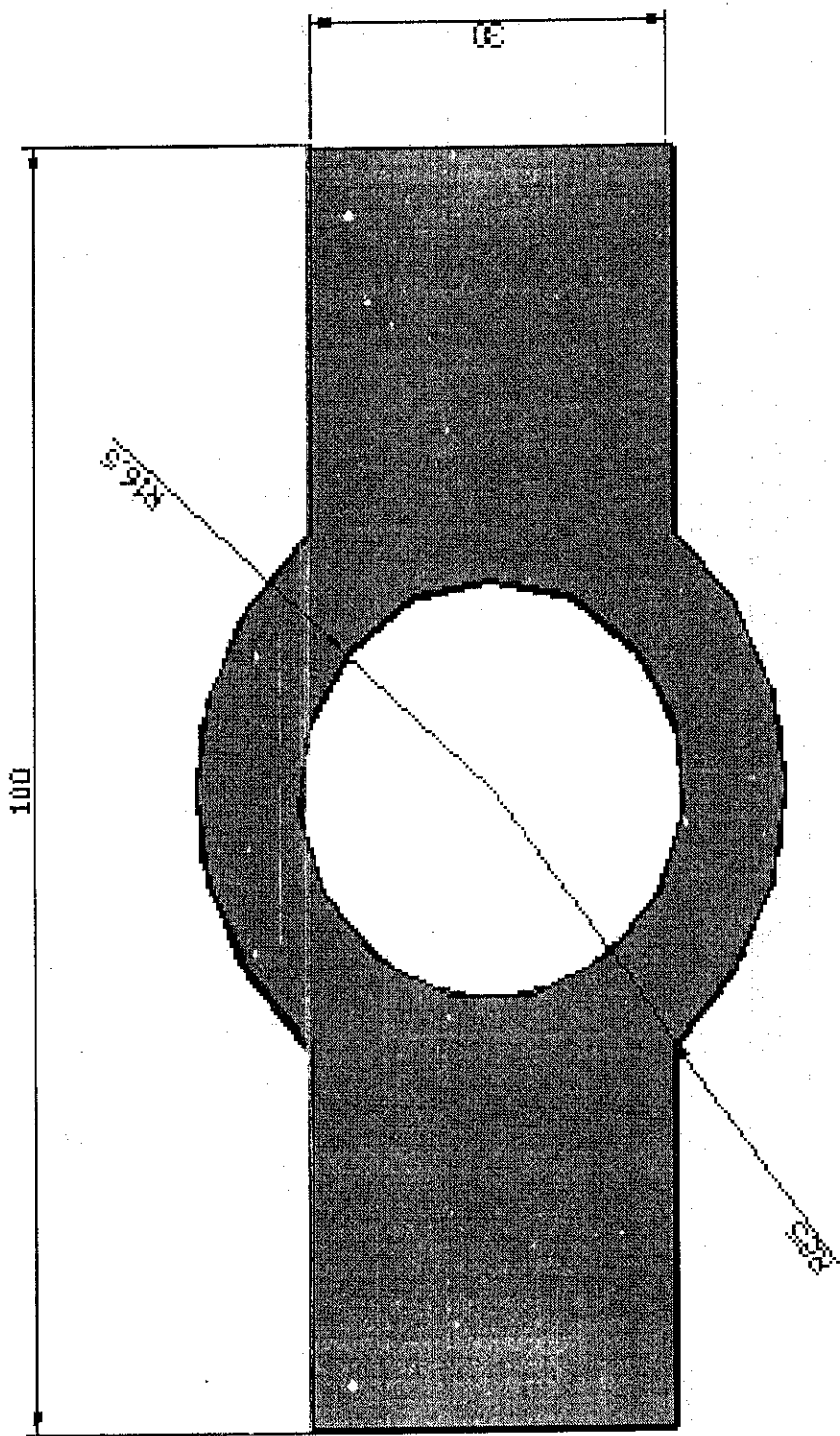
APPENDIX 8: Savonius Rotor Design 3 Top View



APPENDIX 9: Savonius Rotor Design 3 Side View

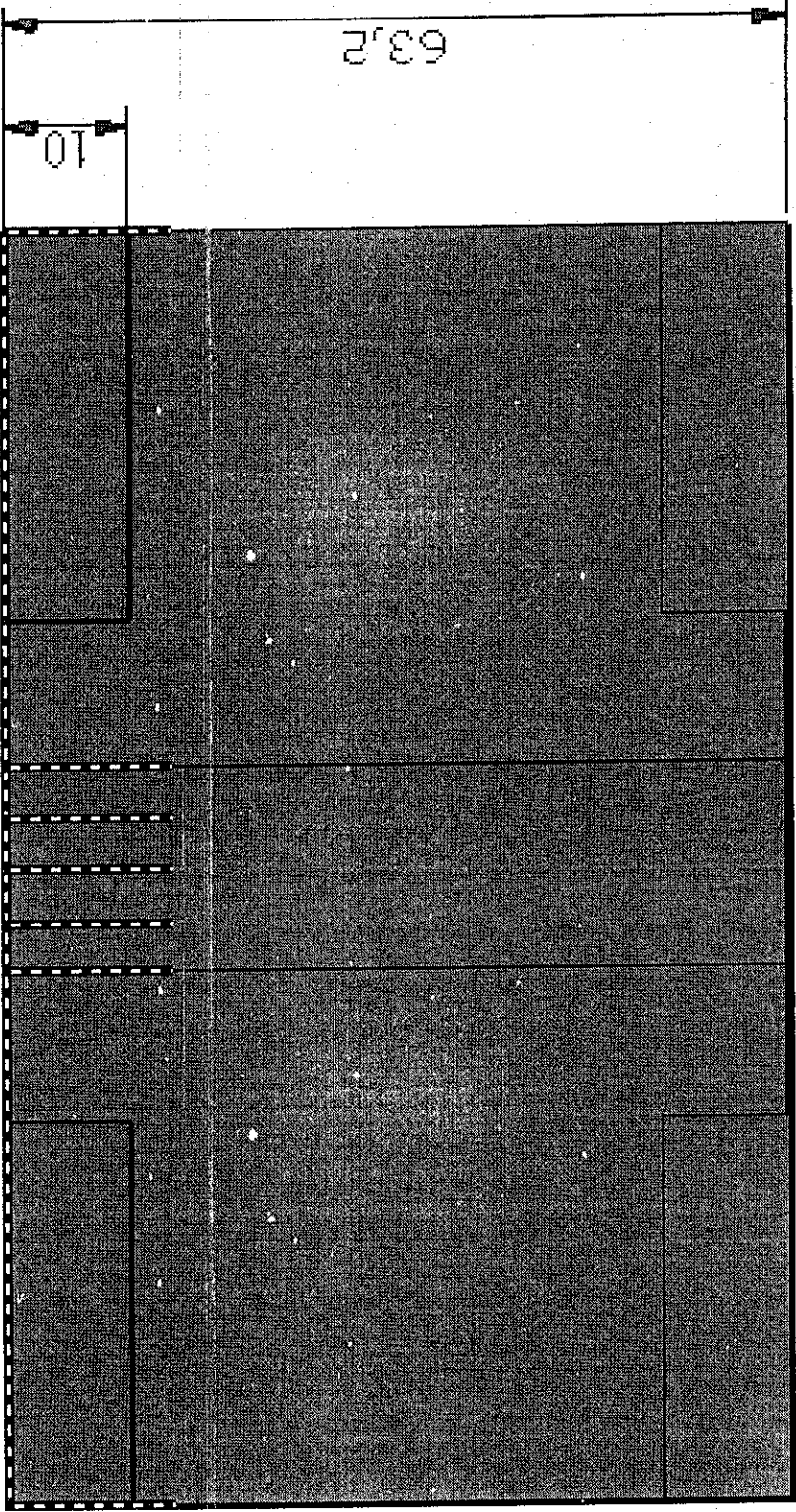


APPENDIX 10: Test Rig Design 1 Partially Bounded Flow 3D View

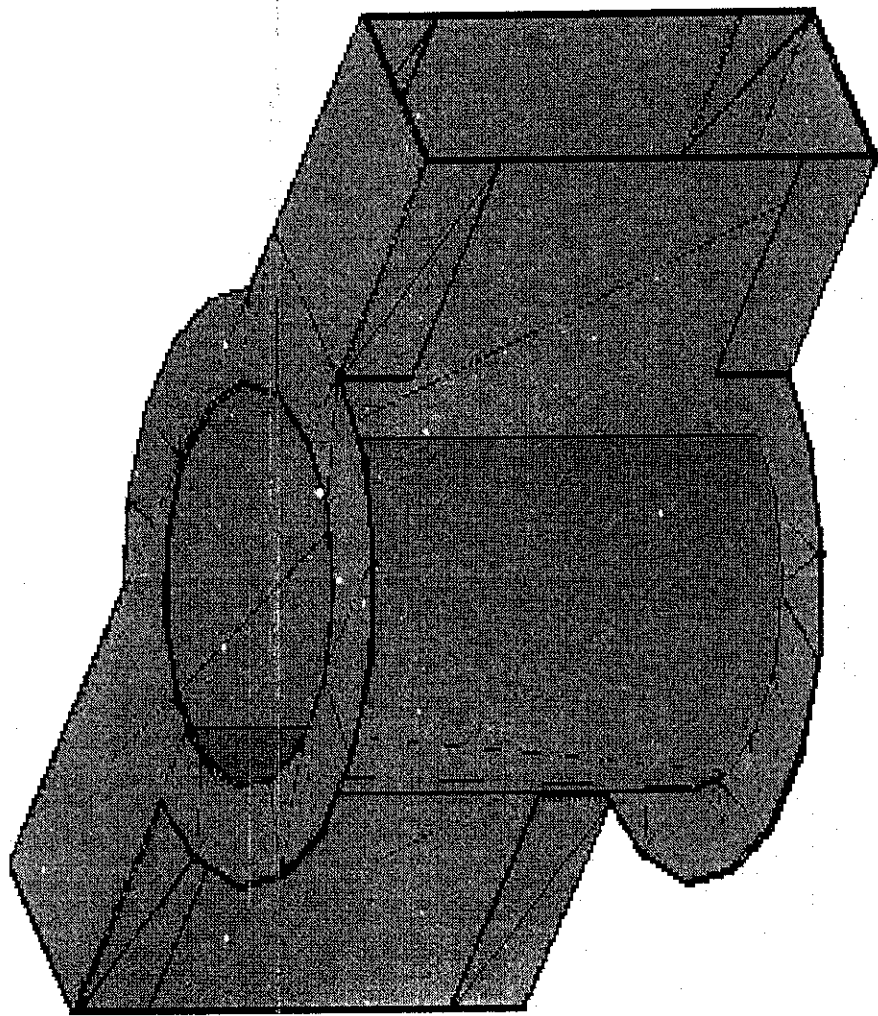


APPENDIX 11: Test Rig Design 1 Partially Bounded Flow Top View

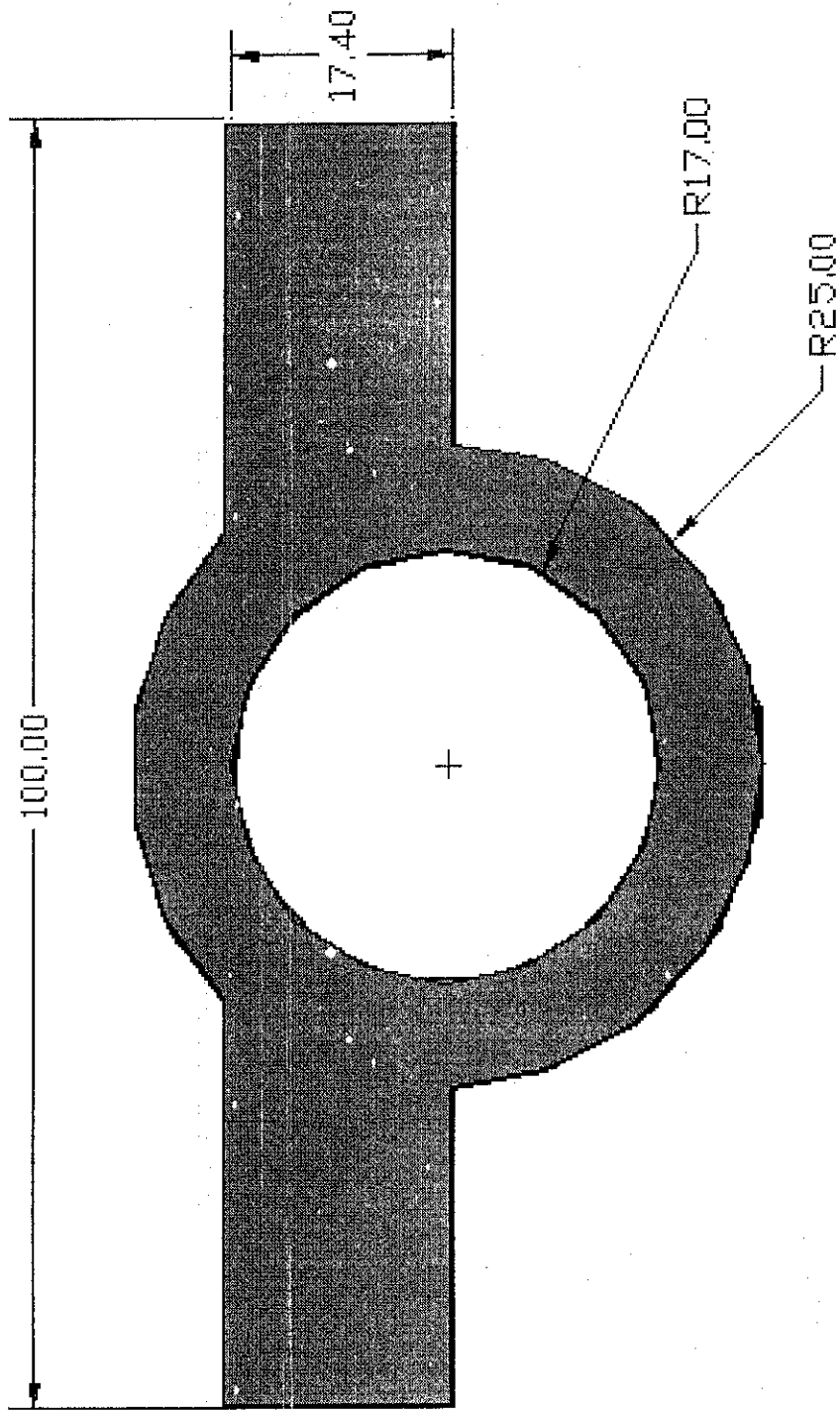
13



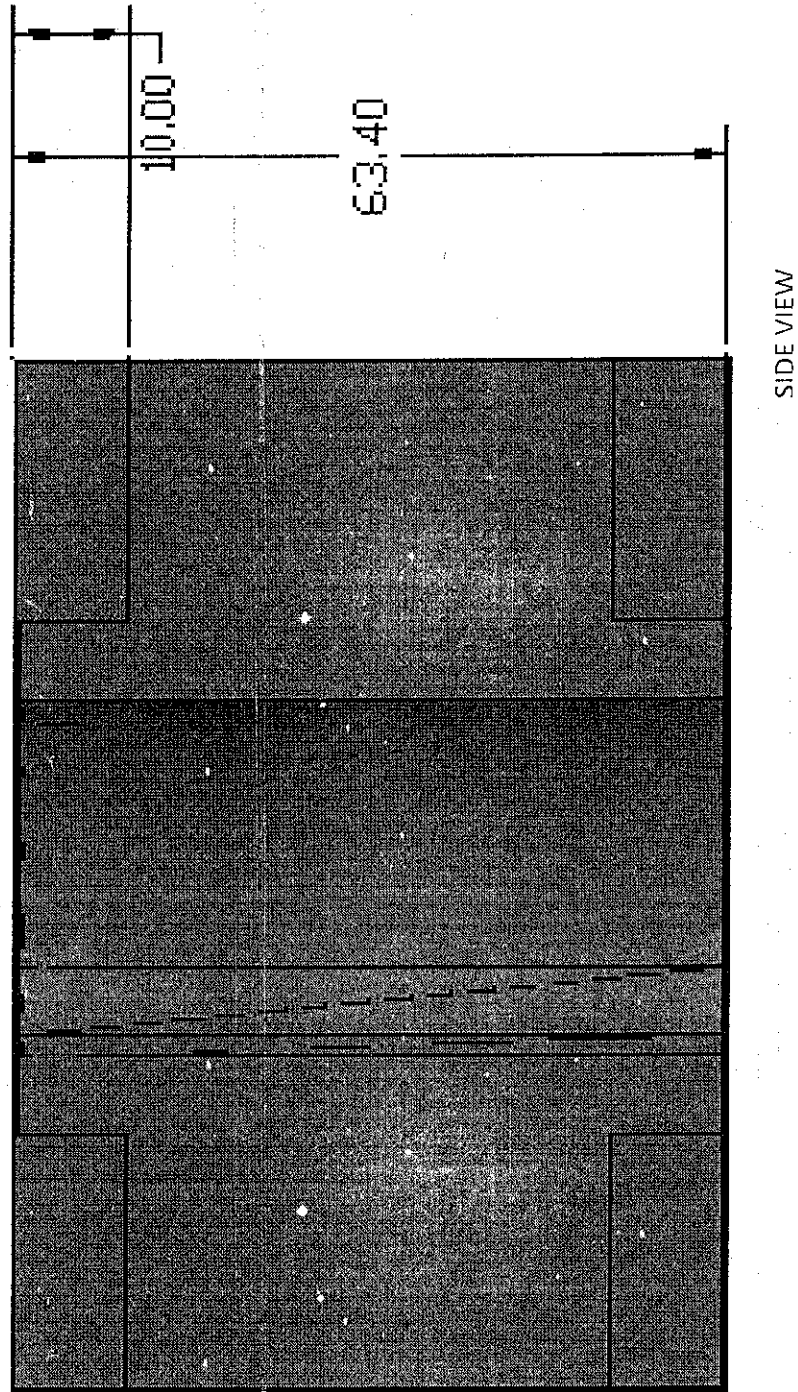
APPENDIX 12: Test Rig Design 1 Partially Bounded Flow Side View



APPENDIX 13: Test Rig Design 2 Fully Bounded Flow 3D View



APPENDIX 14: Test Rig Design 2 Fully Bounded Flow Top View



APPENDIX 15: Test Rig Design 2 Fully Bounded Flow Side View